Synthesis, Reactivity, and Properties of Benz[*a*]azulenes *via* [8 + 2] Cycloaddition of 2*H*-cyclohepta[*b*]furan-2-ones with an Enamine

Taku Shoji,*[a] Akari Yamazaki,[a] Konomi Shimamura,[b] Rina Sakai,[b] Ryuzi Katoh,[b] Masafumi Yasunami,[b†] Tetsuo Okujima,[c] and Shunji Ito[d]

[a] Graduate School of Science and Technology, Shinshu University, Matsumoto 390-8621, Japan. E-mail: tshoji@shinshu-u.ac.jp

[b] Department of Chemical Biology and Applied Chemistry, College of Engineering, Nihon University, Koriyama 963-8642, Japan.

[c] Department of Chemistry and Biology, Graduate School of Science and Engineering, Ehime University, Matsuyama 790-8577, Japan

[d] Graduate School of Science and Technology, Hirosaki University, Hirosaki 036-8561, Japan.

Abstract

Starting with the reaction of 2*H*-cyclohepta[*b*]furan-2-ones with an enamine, which was prepared from 4-*tert*-butylcyclohexanone and pyrrolidine, benz[*a*]azulenes having both formyl and *tert*-butyl groups were obtained in the three-step sequence. Subsequently, both the formyl and *tert*-butyl groups were eliminated by heating the benz[*a*]azulene derivatives in 100% H_3PO_4 to give benz[*a*]azulenes without these substituents in high yields. In terms of the product yield, this method is the best one ever reported for the synthesis of the parent benz[*a*]azulene so far. The conversion of the benz[*a*]azulene derivatives with a formyl group into cyclohept[*a*]acenaphthylen-3-one derivatives was also investigated *via* Knoevenagel condensation with dimethyl malonate, followed by Brønsted acid-mediated intramolecular

cyclization. The structural features including the bond alternation in the benz[*a*]azulene derivatives were revealed by NMR studies, NICS calculations, and a single-crystal X-ray structural analysis. The optical and electrochemical properties of a series of benz[*a*]azulene derivatives were evaluated by UV/Vis, fluorescence spectroscopy and voltammetry experiments. As a result, we found that some benz[*a*]azulene derivatives showed remarkable luminescence in acidic media. In addition, the benz[*a*]azulene derivatives with the electron-withdrawing group and cyclohept[*a*]acenaphthylen-3-one derivative displayed good reversibility in the spectral changes under the electrochemical redox conditions.

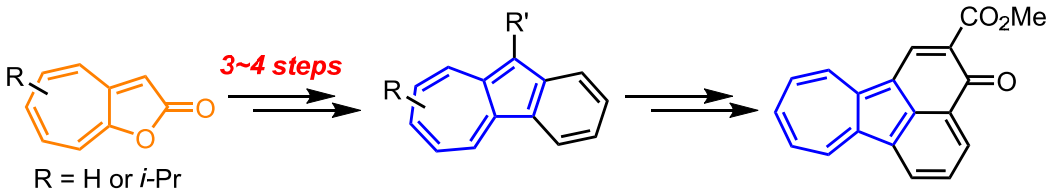

Introduction

Aromatic hydrocarbon skeletons with various functional groups and/or extended π-conjugated systems are expected to be promising resources for novel functional materials with attractive electronic structures. Particularly, polycyclic aromatic hydrocarbons show interesting properties such as near-infrared absorption, reversible redox activity, and high electrical conductivity, and are used in a variety of practical applications such as near-infrared responsive dyes, organic semiconductors, electrodes for rechargeable batteries, and so on.[1]

Azulene is one of the non-alternate aromatic hydrocarbons that has fascinated many chemists because of its unique reactivity and properties.[2] In recent years, the properties of azulene derivatives have been continuously evaluated in various practical applications, such as organic electronics, [3] photovoltaics, [4] electrochromism, [5] and stimuli-responsive materials.[6] Benz[*a*]azulene, a structural isomer of anthracene, is one of polycyclic aromatic

compounds, which has also been of much interest in terms of its structural and optical properties.[7] In this regard, several research groups have reported the preparation of benz[*a*]azulenes and their derivatives for a long time,[8] but the synthetic method for the parent compound is still limited (Scheme 1). To the best of our knowledge, the synthesis of the parent benz[*a*]azulene has firstly been achieved in 1948 by Plattner *et al*.[9] and Treibs,[10] independently, in a similar manner, i.e., the reaction of fluorene with ethyl diazoacetate, but the products yield was not available in the literature. After a while, Wege *et al.* reported the synthesis of benz[*a*]azulene in two or three steps *via* reactive intermediates such as carbene[11] and benzyne[12], but the overall yield was low. In a more practical approach, Hansen and Sperandio reported the preparation of the parent benz[*a*]azulene starting from 2-iodobenzyl alcohol in six steps in an overall yield of 44%,[13] and a year later, the same group continuously evaluated its reactivity, structural and optical properties.[14] However, the yield in the synthesis of the parent benz[*a*]azulene still remains insufficient, and the reactivity, structural and optical properties of itself and its derivatives have not been fully evaluated.

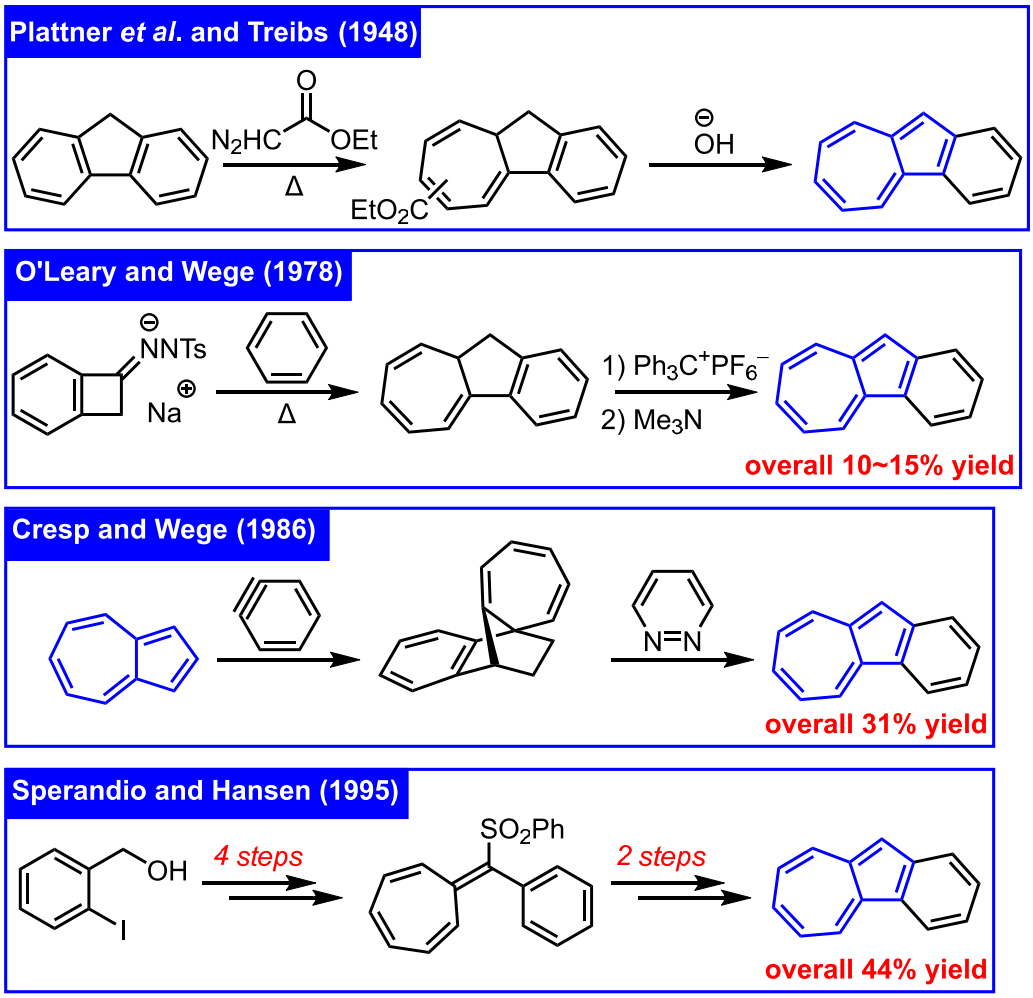

Scheme 1. Synthetic methods for the parent benz[*a*]azulene appeared in the literature.

In this paper, we report an efficient method for the synthesis of benz[*a*]azulenes, which were difficult to synthesize by using previously reported methods, as well as the reactivity of these compounds obtained in this study. As a result, we found that a benz[*a*]azulene derivative can be converted into cyclohept[*a*]acenaphthylen-3-one derivative by several step synthesis. The optical properties of the newly prepared benz[*a*]azulenes and cyclohept[*a*]acenaphthylen-3-one derivative were characterized by UV/Vis and fluorescence spectroscopy. We found that these derivatives exhibit a remarkable spectral change and emission in an acidic solution compared to those under neutral conditions. The electrochemical features of these derivatives have been investigated by both voltammetry and spectroelectrochemical experiments, revealing that some benz[*a*]azulene derivatives

exhibited electrochromism with good reversibility, despite the observation of irreversible cyclic voltammograms.

Results and Discussion

Synthesis of benz[*a*]azulene derivatives

As the first trial of the facile synthesis of benz[*a*]azulenes, we have attempted the conversion of tetrahydrobenz[*a*]azulenes,[15] which are considered as a useful precursor, by the oxidative aromatization reaction using 2,3-dichloro-5,6-dicyano-*p*-benzoquinone (DDQ) as the oxidant (Scheme 2). However, this reaction did not give the desired benz[*a*]azulenes at all, but resulted in only immediate decomposition of the precursors. Thus, it is necessary to develop a new synthetic route for the preparation for benz[*a*]azulenes.

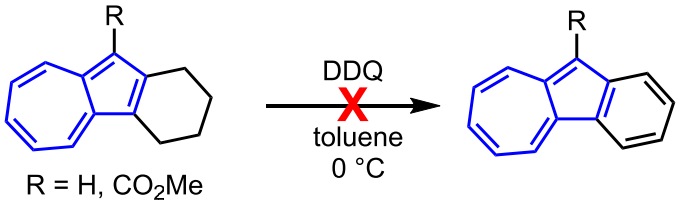

Scheme 2. An attempt to the synthesis of benz[*a*]azulenes by the oxidation with DDQ.

Azulene derivatives are known to form charge transfer complexes with electron-deficient molecules such as picric acid and DDQ.[8b,16] Based on this fact, we believed that the above decomposition was caused by the formation of charge-transfer (CT) complexes, which might take precedence over the oxidation reaction. Based on this hypothesis, we decided to introduce a bulky substituent, a *tert*-butyl group, into the starting materials, tetrahydrobenz[*a*]azulenes, to inhibit the formation of the CT complexes.

As a result of this investigation, we established a four-step synthesis of benz[*a*]azulene derivatives starting from 2*H*-cyclohepta[*b*]furan-2-ones. The overview of the synthetic pathway of the benz[*a*]azulene derivatives appeared in Scheme 3.

Tetrahydrobenz[*a*]azulene **2a** was prepared by the [8 + 2] cycloaddition of **1a** with enamine prepared from 4-*tert*-butylcyclohexanone and pyrrolidine in 87% yield.[17] The reaction of **2a** with DDQ showed remarkable decomposition as described above, so no obvious product was obtained by this reaction. This result was considered as an overreaction in the oxidation reaction owing to the high reactivity of **2a** induced by the higher HOMO level by the condensation of the cyclohexane ring. Therefore, **2a** was transformed by the Vilsmeier reaction to the formyl derivative **3a** in 99% yield, followed by aromatization of **3a** with DDQ as an oxidant at room temperature, resulted in 10-formylbenz[*a*]azulene **4a** in 98% yield. This success may be attributed to the synergistic effect of stabilization of the compound, arising from the moderate electron-withdrawing nature of the formyl group and inhibition of CT-complex formation by the steric hindrance of the substituted *tert*-butyl group. Treatment of **4a** with 100% H_3PO_4 at 140 °C resulted in the one-pot elimination of both the formyl and *tert*-butyl groups to afford **5a** in 71% yield. The overall yield (4 steps, 60%) of this synthetic procedure is the highest one among those of the previously reported synthesis for **5a**. It should also be noted that the simultaneous removal of the formyl and *tert*-butyl groups of **4a** with 100% H_3PO_4 can only be successful under the diluted conditions because the decomposition reaction is more pronounced at the higher concentration. Benz[*a*]azulenes **5b** and **5c** having an isopropyl group at the seven-membered ring in 49% and 41% yields, respectively, could also be prepared in the same manner as in the preparation of **5a**. Heating of **4a** and **4b** in 100% H_3PO_4 for a shorter time (3–4 h) gave **6a** (91%) and **6b** (81%), in which only the *tert*-butyl group was removed. Thus, the elimination of the formyl group should correspond to the rate-determining step in the formation of benz[*a*]azulenes by treatment with 100% H_3PO_4. Vilsmeier reaction of **5a** was also investigated. In this reaction, the reaction did not proceed in the fused benzene ring, yielding **6a** with a formyl group on the azulene moiety in 81% yield. This result implies that the reactivity of the benzene moiety is not significantly improved even when the ring is fused in the electron-rich five-membered

ring of azulene. The carbonyl function attached to the azulene ring at the 1-position is successively reduced to a methylene group by $NaBH_4$ in the presence of $BF_3{\cdot}OEt_2$.[18] Thus, under the similar conditions the formyl group of **4b** was reduced to give **7** with a methyl function at the 10-position in 19% yield (Scheme 3).

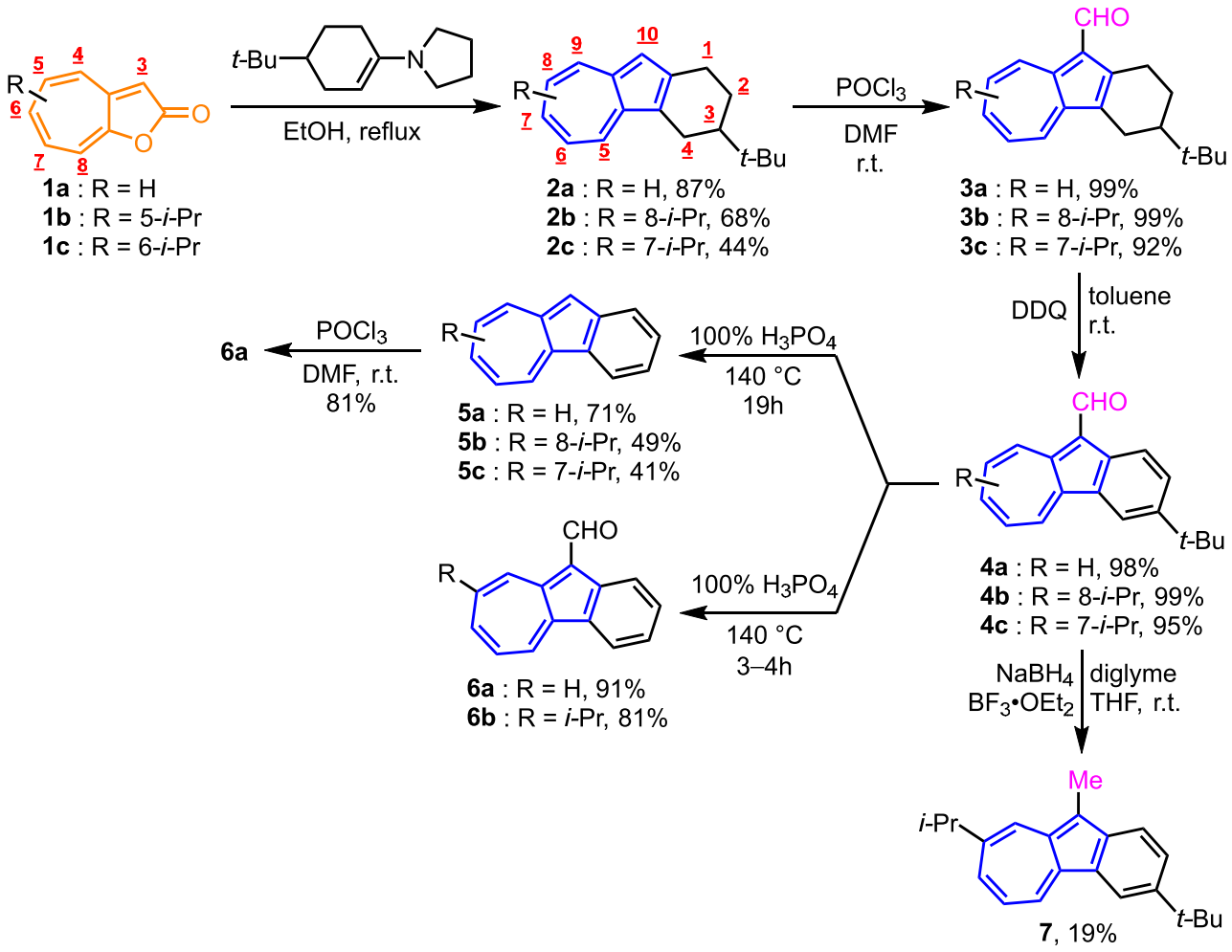

Scheme 3. Synthesis of benz[*a*]azulenes from 2*H*-cyclohepta[*b*]furan-2-ones **1a**–**1c**.

Introduction of various functional groups to benz[*a*]azulene derivatives at the 10-position was also examined to evaluate their reactivity toward electrophiles. Considering both stability and solubility, **2b** with both a *tert*-butyl group at the 3-position and an isopropyl group at the 8-position were selected as starting materials. An overview of the synthetic pathway is illustrated in Scheme 4.

The trifluoroacetylation of **2b** with trifluoroacetic anhydride in $CHCl_3$ and pyridine at

room temperature afforded **8** in 95% yield. In this reaction, the product yield was significantly reduced in the absence of pyridine, probably due to the inactivation towards the electrophilic substitution by the protonation of the substrate. Aromatization of **8** to **9** (86%) was readily established by the oxidation with DDQ. However, unlike the reduction from **4b** to **7**, the reaction of **9** with $NaBH_4$ in the presence of $BF_3{\cdot}OEt_2$ produced diazulenylmethane derivative **10** in 72% yield, instead of a methylene compound. This reaction probably proceeds by a similar mechanism for the formation of diazulenyl- and triazulenylmethane derivatives that we have reported so far.[19]

Benz[*a*]azulene derivative **12** with a methyl ester function was prepared in a two-step yield of 40% by exchanging the trifluoromethyl group of **8** to methoxy function with MeONa in MeOH at the reflux temperature, followed by DDQ-oxidation of the intermediary obtained **11**. Treatment of **12** with 100% H_3PO_4 at 100 °C produced **13**, where only the methyl ester group at the 10-position was removed.

A methyl sulfide group was introduced in three steps from **2b** at the 10-position to synthesize **15**: In the presence of dimethylsulfoxide (DMSO) and trifluoroacetic anhydride (TFAA), **2b** is rapidly converted to the corresponding dimethylsulfonium ion, which is readily eliminated a methyl group upon the treatment with triethylamine to generate **14** in 95% as the two-step yield (to be precise, this reaction is an S_N2 reaction in which triethylamine attacks the methyl group of the dimethylsulfonium ion to eliminate the azulenyl sulfide).[20] The oxidative aromatization of **14** with DDQ proceeded smoothly to afford the desired product **15** in high yield (95%).

The preparation of **18a**,**b** with an aryl group at the 10-position was also established by utilizing the Suzuki-Miyaura cross-coupling. The precursor, the iodo derivative **16**, was prepared by the reaction of **2b** with *N*-iodosuccinimide (NIS) in the presence of a small amount of triethylamine in CH_2Cl_2 as the solvent. However, as similar to the iodoazulenes that we have reported previously, compound **16** was unstable and was used for the next

Suzuki-Miyaura cross-coupling without further purification. Cross-coupling reaction of **16** with phenylboronic acid or 4-*tert*-butylphenylboronic acid in the presence of Pd(dppf)Cl_2 as a catalyst furnished the corresponding products **17a** and **17b** in 84% and 79% yields, respectively. Aromatization of the cyclohexane moiety of **17a** and **17b** to the fused benzene ring was achieved by the treatment with DDQ giving **18a** and **18b**, but the yields became slightly lower due to the competing decomposition (**18a**, 67%; **18b**, 53%). The low yield of the products was probably due to the instability of **18a** and **18b**, showing significant decomposition during the storage under the ambient conditions.

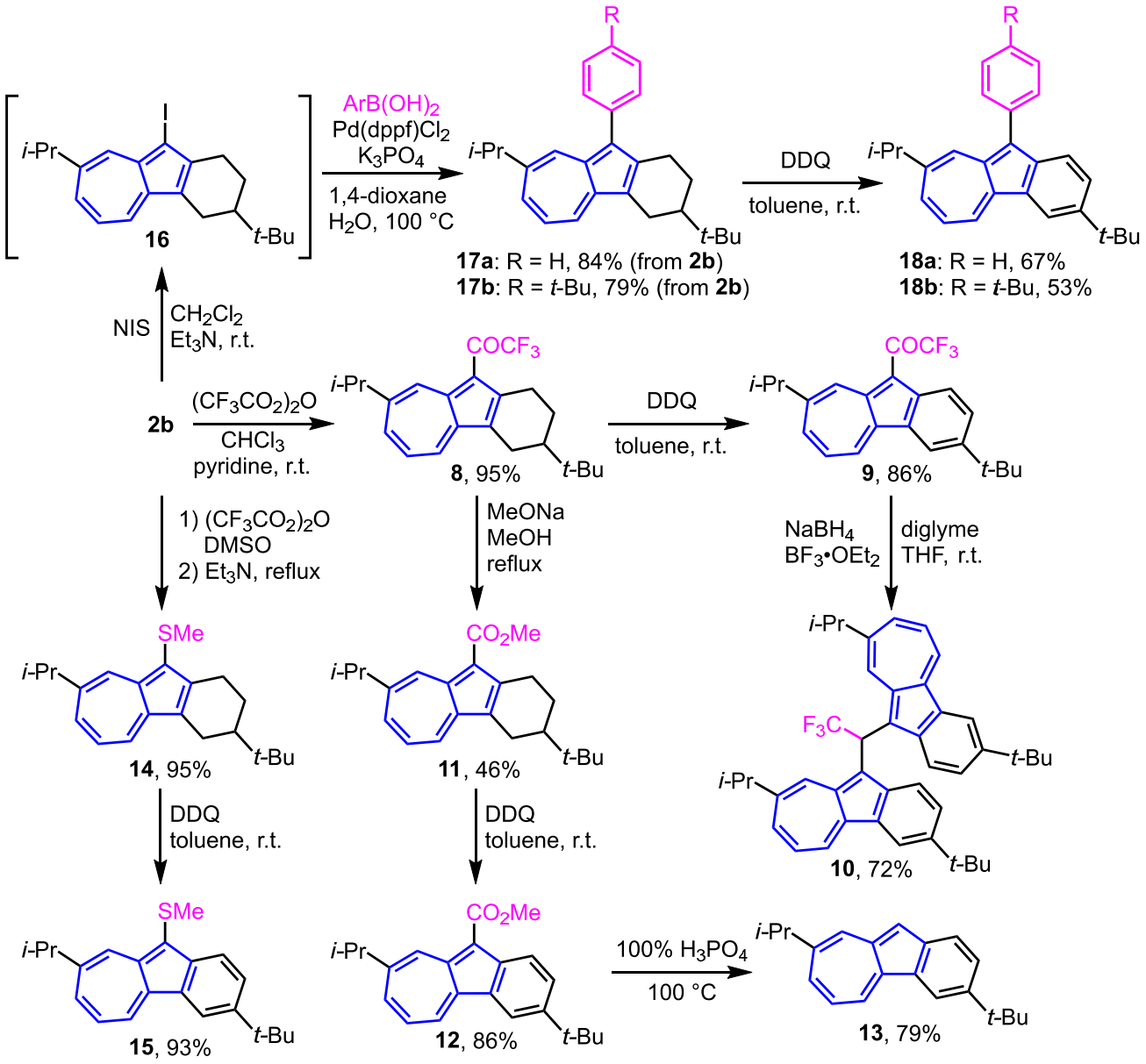

Scheme 4. Synthesis of 3-*tert*-butyl-8-isopropylbenz[*a*]azulene derivatives with various functions at the 10-position.

The aromatization of **19** was unsuccessful by the treatment with DDQ. The ester derivative **19** was found to be converted to **20** by the treatment with NBS in $CHCl_3$, but the product was bromine-substituted at the 3-position (Scheme 5). Furthermore, the compound **20** was transformed to **21** by the decarboxylation reaction by heating in 100% H_3PO_4 at 100 °C, but in rather low yield (21%).

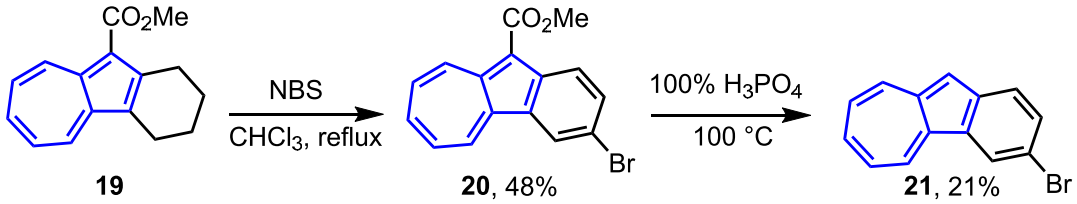

19 **20**, 48% **21**, 21%

Scheme 5. Synthesis of 3-bromobenz[*a*]azulene derivatives **20** and **21**.

Synthesis of cyclohept[*a*]acenaphthylen-3-one derivatives

The expansion of the π-conjugated system is expected to enhance the optical properties based on a decrease in the HOMO-LUMO energy gap of the compound. Thus, the synthesis of cyclohept[*a*]acenaphthylen-3-one, an kind of naphthazulene, was investigated starting from **4a**,**b** and **6a**,**b**. As shown in Scheme 6, we planned a two-step synthesis of cyclohept[*a*]acenaphthylen-3-one *via* Knoevenagel condensation of **4a**,**b** and **6a**,**b** with dimethyl malonate, followed by intramolecular cyclization in the presence of Brønsted acid.

The Knoevenagel reaction of **4b** with malononitrile in the presence of excess alumina catalyst gave the corresponding dicyanovinyl derivatives in 98% yield.[21] Based on the results, the reaction of dimethyl malonate with the formyl derivatives **4a**,**b** and **6a**,**b** was carried out under the similar conditions, but the reaction did not proceed, and the starting

materials were completely recovered. Therefore, the condensation reaction with dimethyl malonate were carried out under general Knoevenagel conditions by using piperidine as a base, resulting in the corresponding vinyl derivatives **23a**,**b** and **24a**,**b** from **4a**,**b** and **6a**,**b** in moderate to good yields. Polyphosphoric acid (PPA) mediated intramolecular cyclization of **4a**,**b** and **6a**,**b** was investigated, but the reaction of **23a**,**b** and **24b** showed the decomposition to afford no identified product. On the other hand, the cyclization reaction of **24a** took place to yield cyclohept[*a*]acenaphthylen-3-one **25** in 36% yield, along with an unidentified mixture. By using Eaton's reagent the reaction produced the same product in an improved yield of 66%. Comparing PPA and Eaton's reagent, the latter has advantages of the improvement of product yield, less formation of an unidentified mixture, and easier purification process. Furthermore, the product **25** obtained by the cyclization reaction with Eaton's reagent can be easily separated by silica gel chromatography, since the unidentified mixture formed by the reaction are highly polar materials, which making it suitable for the preparation of cyclohept[*a*]acenaphthylen-3-one **25** from the viewpoint of the easier purification process.

Compound **25** showed high solubility in water, even though it had no hydrophilic functional group. The high hydrophilicity of **25** should be ascribed to the contribution of bipolar structure involving both azulenium and phenoxide ions as illustrated by the resonance structure of **25'** in Scheme 6. Furthermore, when K_2CO_3 was added to the aqueous solution, crystals of **25** were precipitated immediately, suggesting that the contribution of **25'** was reduced owing to the instability of the azulenium ion form under the basic conditions.

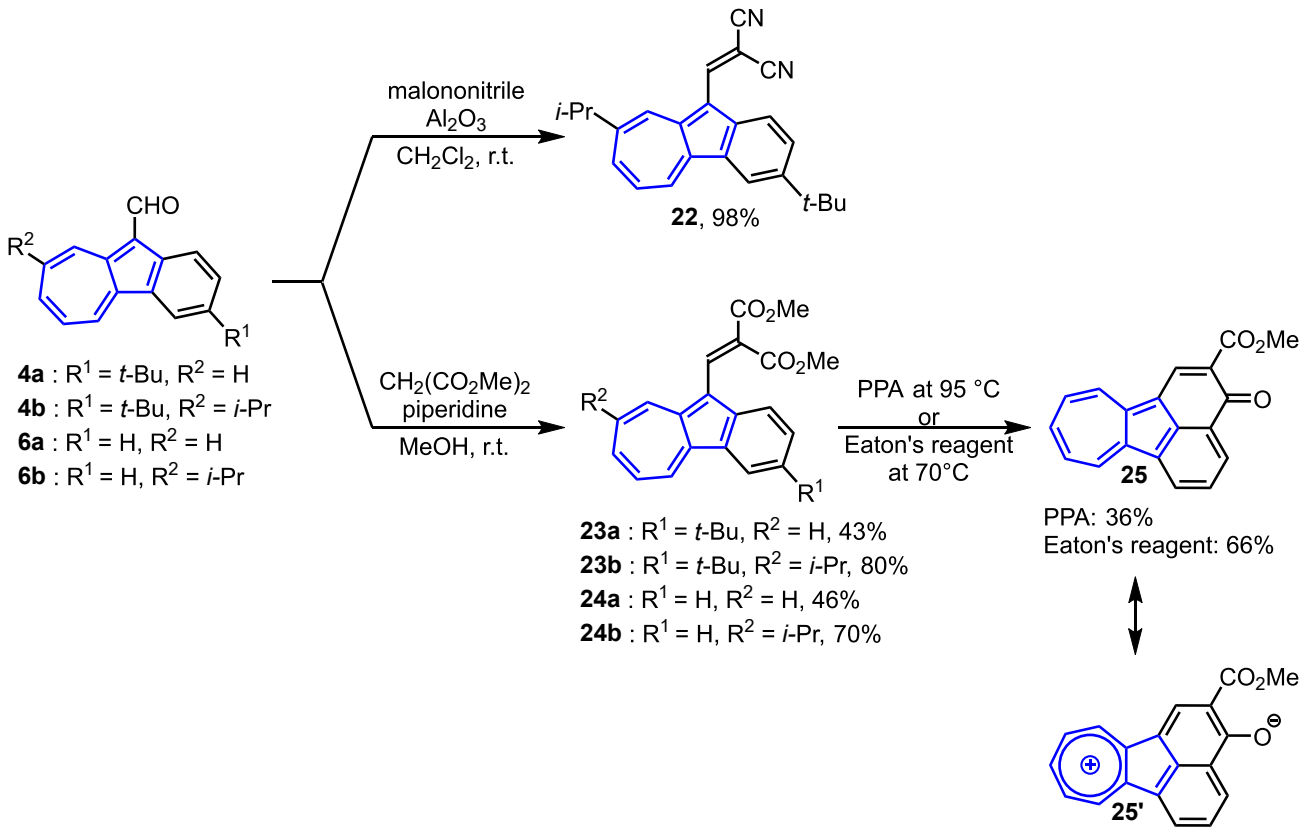

Scheme 6. Knoevenagel reaction of **4a**,**b** and **6a**,**b**, and the synthesis of cyclohept[*a*]acenaphthylen-3-one derivative **25**; PPA = polyphosphoric acid, Eaton's reagent = 7.7 wt.% phosphorus pentoxide in methanesulfonic acid.

Spectroscopic Properties

All the new compounds prepared in this study were well characterized on the basis of spectral data as described in the experimental section. High-resolution mass spectra of the reported compounds ionized by MALDI-TOF showed the correct molecular ion peaks. The assignment of the proton signals of the compounds observed in the ^{1}H NMR spectra was confirmed by COSY experiments. Benz[*a*]azulenes prepared in this study showed the pronounced bond-length alternation at the seven-membered ring. This manifested itself as a difference in the coupling constants in the ^{1}H NMR spectra as shown in Figure 1. For example, the coupling constants $^{3}J(H^{5},H^{6})$ and $^{3}J(H^{7},H^{8})$ at the seven-membered ring of **5a** are both J = 8.3 Hz, suggesting that these parts exhibit single bond characters. On the other

hand, a large coupling constant of J = 11.0 Hz was observed between the vicinal protons H^6-H^7 and H^8-H^9, showing the double bond characters of these parts. Similar bond-length alternations were also observed in the ^{1}H NMR spectra of **5b** and **13**. Therefore, these observations indicate that the aromaticity of the azulene moiety of benz[*a*]azulenes is reduced by the fused benzene ring in the five-membered ring.

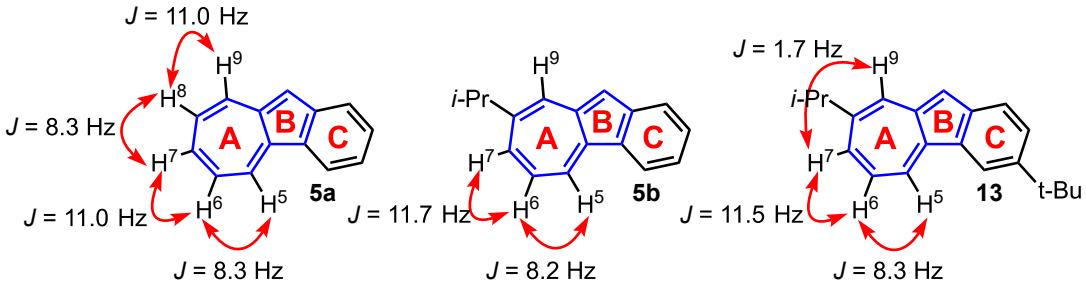

Figure 1. Coupling constants of each proton observed by ^{1}H NMR spectra of **5a**, **5b**, and **13**.

To clarify the aromaticity for each ring of **5a**, **5b**, and **13** in terms of theoretical calculations, nucleus-independent chemical shift (NICS) calculations were performed at the GIAO/HF/6-311+G(d,p) level. The NICS(0) and NICS(1) values for **5a**, **5b**, and **13**, and those of the parent azulene calculated in the same level as a reference are summarized in Table 1. The NICS(0) and NICS(1) values for A and B rings of **5a**, **5b**, and **13** showed distinct down-field shifts compared to those of the parent azulene. For example, the seven-membered A ring of **5a** exhibited the values of −2.92 ppm for NICS(0) and −5.50 ppm for NICS(1), which are lower than those of the parent azulene [NICS(0) = −8.25 ppm, NICS(1) = −9.90 ppm]. Thus, these results confirm that the seven-membered A ring shows the reduced aromaticity as predicted from the ^{1}H NMR experiments. The lower aromaticity of the azulene moieties of **5a**, **5b**, and **13**, relative to that of parent azulene, should be accounted by the less contribution of the more unstable *ortho*-quinoid structures in the resonance form in order to retain the aromaticity of the fused benzene ring (Scheme 7).

Table 1. The NICS(0) and NICS(1) of **5a**, **5b**, and **13**, and those of azulene as a reference at the GIAO/HF/6-311+G(d,p) level

ring	NICS (X)	**5a**	**5b**	**13**	Azulene
A	1	−5.50	−5.33	−4.77	−9.90
	0	−2.92	−2.83	−2.21	−8.25
B	1	−12.73	−11.79	−11.37	−21.03
	0	−11.32	−10.25	−9.74	−21.55
C	1	−12.43	−12.25	−12.46	–
	0	−11.07	−10.91	−11.32	–

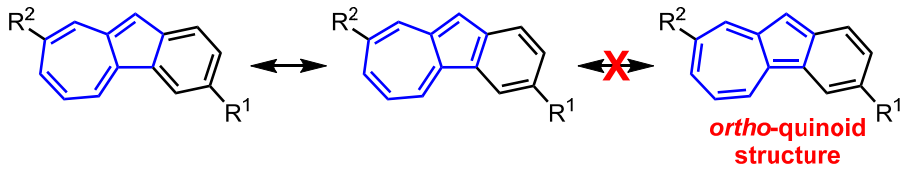

Scheme 7. Plausible resonance structures of **5a**, **5b**, and **13**.

The suitable single crystal of **6a** was obtained from $CHCl_3$/MeOH mixed solvent by slow evaporation. Thus, the structure of **6a** was confirmed by X-ray structural analysis (Figure 2). Similar to the benz[*a*]azulene derivatives reported so far,[22] the alternating arrangement of long and short bonds, i.e., bond-length alternation, was identified in the seven-membered ring of **6b** by the X-ray structural analysis. The analysis also revealed that the complete planarity in the structure of **6b** and the oxygen atom of the formyl group was oriented toward the H^9 proton side. Furthermore, the H^9 proton signal of **6b** showed a remarkable downfield shift in the ^1H NMR spectrum, suggesting the presence of the intramolecular hydrogen bond between the H^9 proton and the carbonyl oxygen atom.

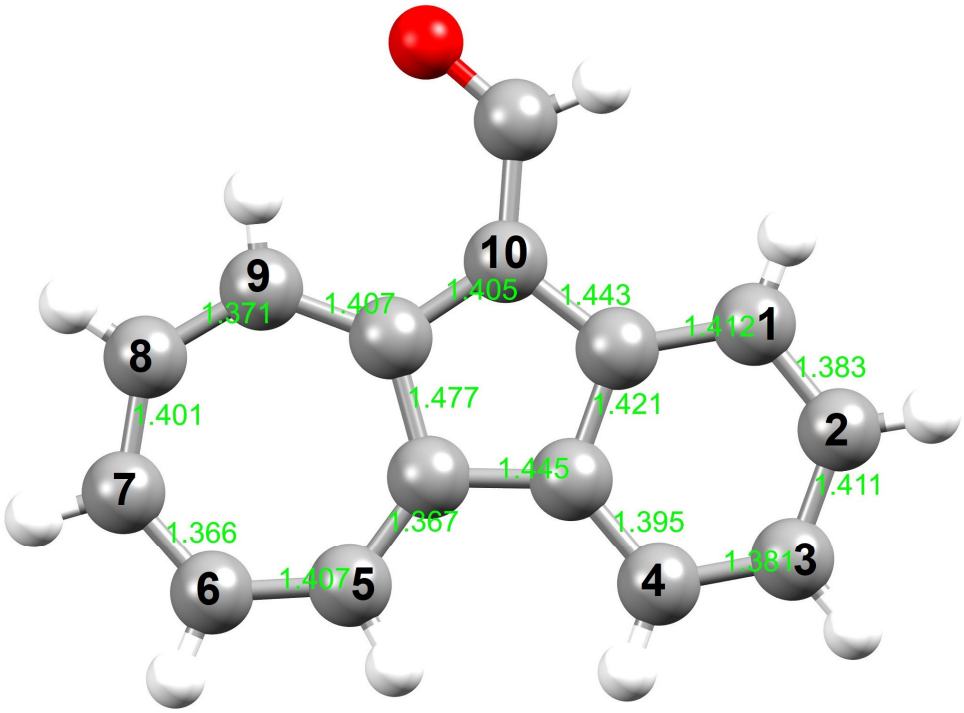

Figure 2. Crystal structure and bond lengths of **6b** (CCDC 1959815).[23]

Absorption maxima and their coefficients in the visible region of benz[*a*]azulenes in CH_2Cl_2 and in 10% CF_3CO_2H (TFA)/CH_2Cl_2 are summarized in Table 2. Most of the derivatives displayed the absorption bands at around 600 nm originating from the π-π* transition of azulene ring itself, whereas their maximal absorption wavelengths depended on the electronic nature of the substituted functional groups. The maximal absorption wavelengths of the most benz[*a*]azulene derivatives displayed a bathochromic shift compared to that of the parent azulene (λ_{max} = 574 nm in CH_2Cl_2), attributed to the extension of the conjugated system due to the fused benzene ring.

Table 2. Absorption Maxima and Their Coefficients in the Visible Region of benz[*a*]azulenes in CH_2Cl_2 and in 10% TFA/CH_2Cl_2.

Sample	λ_{max} (log ε)[a] in CH_2Cl_2	λ_{max} (log ε) in 10% TFA/CH_2Cl_2
4b	434 (3.99), 540 (2.81), 586 (2.82)	390 (4.21), 430 sh (3.96)

5a	381 (3.65), 402 (3.47), 561 (2.69), 612 (2.70), 673 (2.60)	398 (4.37)
5b	380 (3.71), 401 (3.48), 568 (2.66), 616 (2.68), 679 (2.54)	397 (4.48)
5c	383 (3.70), 402 (3.45), 501 (2.69), 548 (2.77), 592 (2.78)	397 (4.46)
7	386 (3.69), 408 (3.50), 590 (2.70), 645 (2.71)	412 (4.31)
9	454 (4.04)	406 sh (4.07), 474 sh (3.61)
10	388 (3.61), 409 (3.51), 573 (2.66), 623 (2.66)	406 (4.14)
12	406 (3.82), 427 (3.85), 536 (2.86), 591 (2.85)	410 (4.23)
13	382 (3.73), 402 (3.47), 570 (2.74), 628 (2.78), 699 (2.70)	406 (4.38)
15	392 (3.58), 414 (3.49), 580 (2.48), 627 (2.49)	401 (4.00)
18a	393 (3.80), 416 (3.70), 587 (2.73), 642 (2.75)	420 (4.18)
18b	418 (3.67), 543 (2.55), 591 (2.59), 657 (2.63)	388 (4.17), 434 sh (3.97)
22	389 (4.16), 507 (4.36)	391 (4.18), 515 (4.27)
23b	447 (4.00), 582 (2.80), 633 (2.75)	385 (4.11), 449 (3.82)
25	383 (4.19), 488 (4.17), 522 (4.32)	481 (4.27)

[a] Shoulder peaks are omitted for clarity.

In the visible region, compound **5a** showed absorption maximum at λ_{max} = 612 nm with the largest molar absorption coefficient in the visible region (Figure 3). The absorption maximum of the UV/Vis spectra of **5b** (λ_{max} = 616 nm) and **5c** (λ_{max} = 592 nm) with an isopropyl group showed bathochromic shift by only 4 nm for the former and hypsochromic shift by 20 nm for the latter, respectively, compared to that of **5a**. On the other hand, the UV/Vis spectrum of **13** (λ_{max} = 628 nm), which has both an isopropyl and a *tert*-butyl groups,

displayed an absorption band at the longest wavelength region among that of **5a**–**5c** and **13**.

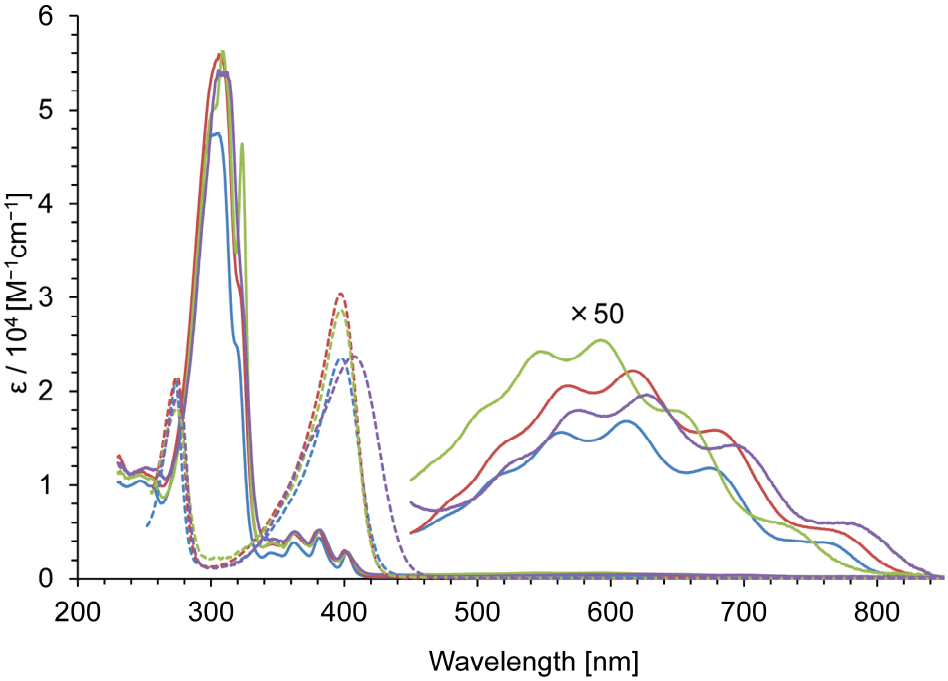

Figure 3. UV/Vis spectra of **5a** (blue line), **5b** (red line), **5c** (light-green line) and **13** (purple line) in CH_2Cl_2 (solid line) and in 10% TFA/CH_2Cl_2 (dotted lines); The spectrum in the visible region in CH_2Cl_2 is magnified ×50.

The effect in the absorption wavelength by the substituents on the azulene ring can be explained by an empirical rule proposed by Plattner et al. in the early days of azulene chemistry.[24] According to this rule, an alkyl group substituted at the odd-numbered positions (i.e., 1-, 3-, 5-, or 7-positions) of the azulene ring shows a red-shift in the absorption maximum in the UV/Vis spectrum, compared to that of the parent azulene. Conversely, the substitution of an alkyl group at the even-numbered positions (i.e., 2-, 4-, 6-, and 8-positions) exhibits a hypsochromic shift in the absorption maximum. Extending this principle, when the electron-withdrawing group is substituted at the odd-numbered position of the azulene ring, the absorption maximum is hypsochromic, and vice versa with the electron-donating group. Plattner's rule was also found to be applicable to benz[*a*]azulenes (Figure 4); a bathochromic shift of the absorption maximum was observed for **7** and **18a**,**b** with methyl

and aryl groups, compared that of **13**. Contrary, the absorption maximum of **9** and **12**, where trifluoroacetyl and ester groups were substituted, showed a hypsochromic shift, compared to that of **13**.

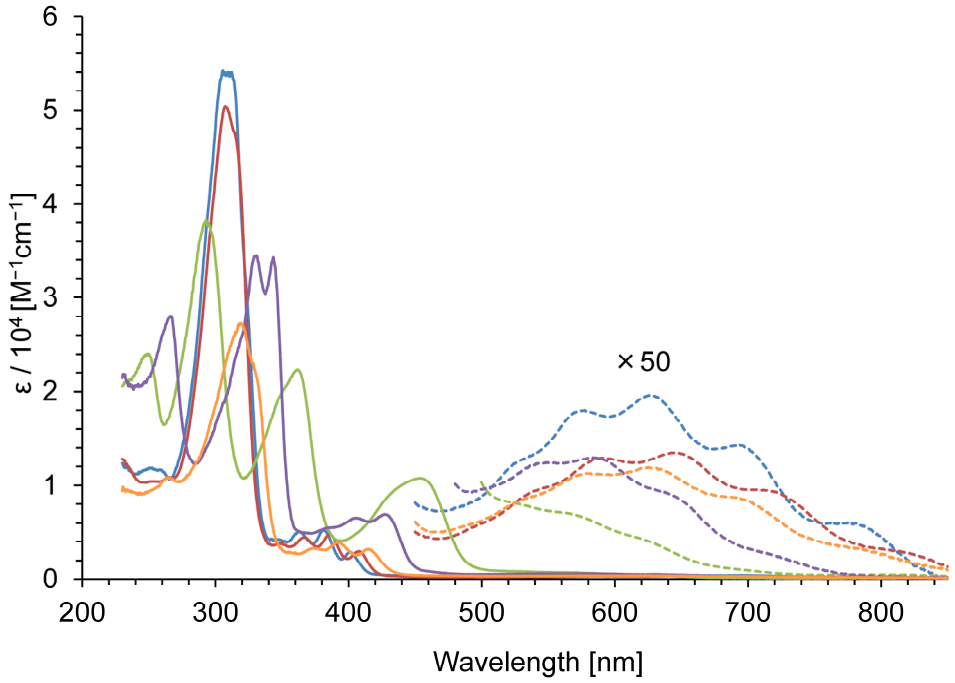

Figure 4. UV/Vis spectra of **7** (red line), **9** (light-green line), **12** (purple line), **13** (blue line), and **15** (orange line) in CH_2Cl_2; The spectrum in the visible region in CH_2Cl_2 is magnified ×50.

The compound **22** with a dicyanovinyl group presented a broad and strong absorption band in the visible region centered at λ_{max} = 515 nm originating from its push-pull structure. Similarly, **23b** showed a relatively strong absorption band at around λ_{max} = 449 nm, but its molar absorption coefficient was smaller than that of **22**. This result could be attributed to the less effective intramolecular charge transfer in **23b**, compared with that of **22**, since the electron-withdrawing nature of the ester group is lower than that of the cyano group. In contrast to the usual azulene derivatives, cyclohept[*a*]acenaphthylen-3-one derivative **25** showed a strong absorption band, where the end absorption reached to the near-infrared region.

Under acidic conditions, azulene derivatives are known to exhibit the color change associated with the formation of azulenium ions.[25] Most of benz[*a*]azulenes prepared in this study change in the absorption bands, which was observed in the UV/Vis spectra in the acidic medium as compared to that in CH_2Cl_2. The compound of **5a** developed a new absorption band at λ_{max} = 398 nm on the UV/Vis spectrum in 10% TFA/CH_2Cl_2 solution. And then the absorption band in the visible region arising from the azulene derivatives observed in CH_2Cl_2 disappeared (Figure 3). The absorption maximum in the visible region of **5b** (λ_{max} = 397 nm) and **5c** (λ_{max} = 397 nm) was almost identical to that of **5a**, while **13** bearing a *tert*-butyl group at the 3-position exhibited a slight bathochromic shift (λ_{max} = 406 nm). Comparing the absorption spectra of a series of 3-*tert*-butyl-8-isopropylbenz[*a*]azulenes with a function at the 10-position in 10% TFA/CH_2Cl_2, there were no considerable differences among each other, implying that the electronic properties of the substituent at the 10-position are not significantly responsible for their absorption wavelengths.

For the detailed study of the protonated species, ^{1}H NMR of **13** was measured in both $CDCl_3$ and 10% $CF_3CO_2D/CDCl_3$. The ^{1}H NMR spectrum of **13** in 10% $CF_3CO_2D/CDCl_3$ showed the disappearance of the proton signal at the 10-position due to the proton-deuterium exchange reaction with CF_3CO_2D. The chemical shifts of all proton signals in the azulene moiety of **13** shifted to the downfield in 10% $CF_3CO_2D/CDCl_3$, compared to those in $CDCl_3$, but the chemical shifts in the fused-benzene ring were not significantly affected. Furthermore, the bond-length alternation of the azulene moiety observed in $CDCl_3$ was disappeared in acidic media attributed to the formation of aromatic tropylium ionic substructure. That is, the azulenium ionic species produced in the acidic medium is given by the structure in Figure 5 (bottom).

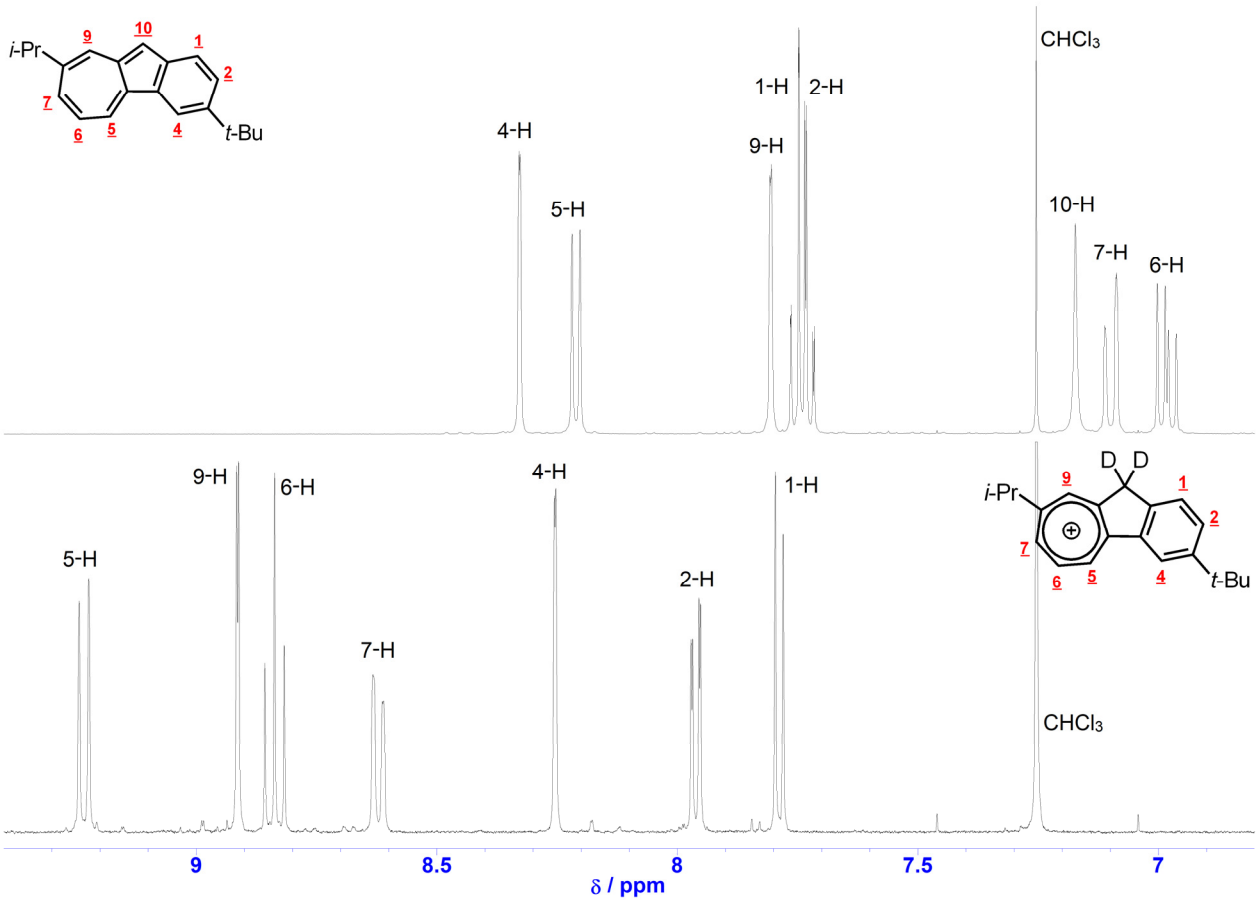

Figure 5. ^{1}H NMR spectra of **13** in $CDCl_3$ (top) and 10% $CF_3CO_2D/CDCl_3$ (bottom).

Azulene derivative does not represent luminescence from the $S_1 \rightarrow S_0$ transition due to the rapid internal conversion in the S_1 state, but in contrast to Kasha's rule, anomalous luminescence from the $S_2 \rightarrow S_0$ transition is observed.[26] However, it is difficult to observe visually because the light emission is very weak. Recently, several researchers, including our group, have reported that azulene derivatives exhibit relatively strong fluorescence under acidic conditions due to the formation of azulenium ions by the protonation of the azulene ring.[27] Previously, Yamaguchi, Yasunami, and their co-workers investigated the luminescence behavior of **5b**, **5c**, **13**, and **21** in cyclohexane. In the study, they found that these derivatives exhibit weak fluorescence from the $S_2 \rightarrow S_0$ transition, similar to that of normal azulenes, with a quantum yield (Φ_{flu}) of 0.038 to 0.13%.[28] In contrast to the results of

Yamaguchi and Yasunami *et al*., we found that a series of benz[*a*]azulene derivatives in acidic medium (i.e., 10% TFA/CH_2Cl_2) exhibit relatively stronger emission and higher quantum yields than in a neutral state.

The emission wavelengths of **5a**, **5b**, **5c**, and **13** showed slight differences; **5b** (λ_{flu} = 446 nm) and **5c** (λ_{flu} = 443 nm) with an isopropyl group at the seven-membered ring exhibited a slight hypsochromic shift of the emission maximum compared to that of **5a** (λ_{flu} = 459 nm), while the opposite phenomenon was detected for **13** (λ_{flu} = 493 nm) with a *tert*-butyl group at the 3-position. These results indicate that the *tert*-butyl group at the 3-position is responsible for the bathochromic shift of the emission wavelength. On the other hand, the substituent at the 10-position of the benz[*a*]azulene skeleton had a significant negative effect on the quantum yield (Φ_{flu}), except for **13**. For example, the fluorescence quantum yields of the formyl derivative **4b** (Φ_{flu} < 1%) and the ester derivative **12** (Φ_{flu} < 1%) were much lower than that of **13** (Φ_{flu} = 10.0%), and their values were below the measurement limit of the instrument. The derivatives other than **4b** and **12** also resulted in lower quantum yields than that of **13**, probably due to non-radiative deactivation by rotation or vibration of the substituent at the 10-position. The emission maxima of **18a** (λ_{flu} = 506 nm) and **18b** (λ_{flu} = 550 nm) with an aryl group displayed a bathochromic shift compared to that of **13**, which may be ascribed to a decrease in the energy gap between the excited and ground states due to the expansion of the conjugated system. Furthermore, **18b** was shifted the emission wavelength to a longer wavelength region than that of **18a**, indicating that the substituent at the *para*-position of the benzene ring may affect the electronic properties of the molecule.

Table 3. Fluorescent properties of benz[*a*]azulenes in 10% TFA/CH_2Cl_2.

Sample	λ_{flu} (λ_{ex}) in 10% TFA/CH_2Cl_2	Φ_{flu} [%]	τ_{flu} [ns]
4b	498 (371)	< 1	1.0

5a	459 (398)	7.4	2.6
5b	446 (397)	13.0	2.9
5c	443 (397)	10.0	2.4
7	490 (412)	8.7	5.0
9	492 (366)	2.6	5.3
10	490 (406)	4.6	5.2
12	489 (410)	< 1	0.9
13	493 (407)	10.0	5.1
15	464 (402)	1.5	5.5
18a	506 (423)	5.0	7.0
18b	550 (388)	4.4	5.0
22	483 (416)	1.3	5.0
23b	531 (385)	2.3	2.0
25	553 (481)	6.0	6.0

Electrochemical properties

As mentioned in the Introduction section, benz[*a*]azulene derivatives have been prepared by various researchers, however, their electrochemical properties have not yet been evaluated. Our group has previously reported that diazuleno[2,1-*a*:1,2-*c*]naphthalenes, an analog of benz[*a*]azulene, exhibits reversible redox waves on cyclic voltammograms.[29] Therefore, the benz[*a*]azulene derivatives prepared in this study may also show the reversible redox wave based on the stabilization of the radical species generated by the electrochemical reactions. Thus, to clarify the electrochemical behavior, redox potentials of benz[*a*]azulenes were measured by cyclic voltammetry (CV) and differential pulse voltammetry (DPV). The redox potentials of these compounds determined by DPV are summarized in Table 4.

Table 4. Redox Potentials[a] of benz[*a*]azulenes determined by DPV.

Sample	E_1^{ox} [V]	E_2^{ox} [V]	E_1^{red} [V]	E_2^{red} [V]
4b	+0.68	–	−1.49	–
5a	+0.44	–	−1.79	–
5b	+0.37	–	−1.83	–
5c	+0.42	+0.63	−1.90	–
7	+0.25	–	−1.95	–
9	+0.85	–	−1.36	–
10	+0.46	+0.63[b]	−1.83	–
12	+0.64	–	−1.62	−1.94
13	+0.32	+0.56	−1.88	–
15	+0.29	+0.66[c]	−1.79	–
18a	+0.39	+0.96	−1.83	–
18b	+0.36	+0.89[d]	−1.87	–
22	+0.76	+1.56	−1.23	−1.94
23b	+0.52	+1.45	−1.48	−1.94
25	+0.82	–	−1.13	−1.93

[a] V vs $Ag/AgNO_3$, 1 mM in benzonitrile containing Et_4NClO_4 (0.1 M), Pt electrode (internal diameter = 1.6 mm), scan rate = 100 mVs^{-1}, and external reference (Fc/Fc^+ = +0.15 V); [b] E_3^{ox} was observed at +0.79 V. [c] E_3^{ox} was observed at +1.12 V. [d] E_3^{ox} was observed at +1.32 V.

Contrary to our predictions, most of benz[*a*]azulenes exhibited irreversible reduction waves on CV, indicating the formation of unstable cation or anion species under the electrochemical oxidation or reduction conditions. Relatively high reversibility was observed

under the electrochemical oxidation conditions of **15**, **18a**, and **18b**. Previously, we have reported that 1-azulenyl sulfides show the reversible redox waves originating from the one-electron oxidation of sulfur atom was observed under the oxidation conditions on CV.[20] The relatively high reversibility of the redox wave for **15** should be attributed to the one-electron oxidation of the sulfur atom, since the half-wave potential under the oxidation conditions is similar to those of 1-azulenyl sulfides reported by us, previously. Whereas the reversible waves under the electrochemical oxidation conditions observed in **18a** and **18b** might be explained by the delocalization of the generated radical cationic species which were stabilized by the extension of the conjugation by the substituted aryl group.

Most of benz[*a*]azulenes showed irreversible redox waves on CV. Especially, **9** and **22** with an electron-withdrawing group exhibited large differences in the redox waves between anodic (E_{pa}) and cathodic (E_{pc}) processes under the reduction conditions, which might be ascribed to changes in the molecular conformation or subsequent reaction of the radical ionic species generated by the redox reaction. If the cause of the irreversibility of the cyclic voltammogram is the slow electron transfer and/or the structural change of the molecule caused by the redox reaction, the reversibility can be improved by reducing the scan rate. On the other hand, if the irreversibility is due to the instability of the generated radical ions, it is expected that the reversibility will be improved by increasing the scan rate (Figure 6). Therefore, the electrochemical reduction of **22** was measured by CV at different scan rates, but the reversibility of the redox wave was not improved in any case.

A continuous measurement of 40 cycles of CV for **22** was also investigated. If the redox reaction are produced new species, the voltammograms should change gradually from the first cycle. However, there was no significant difference between the first and 40th cycles of the voltammogram in the case of **22** (Figure 7). These results indicate the series of the redox reactions regenerate eventually the neutral species of **22**. The regeneration of the neutral species was also supported by the results obtained by the spectroelectrochemical

measurements described later.

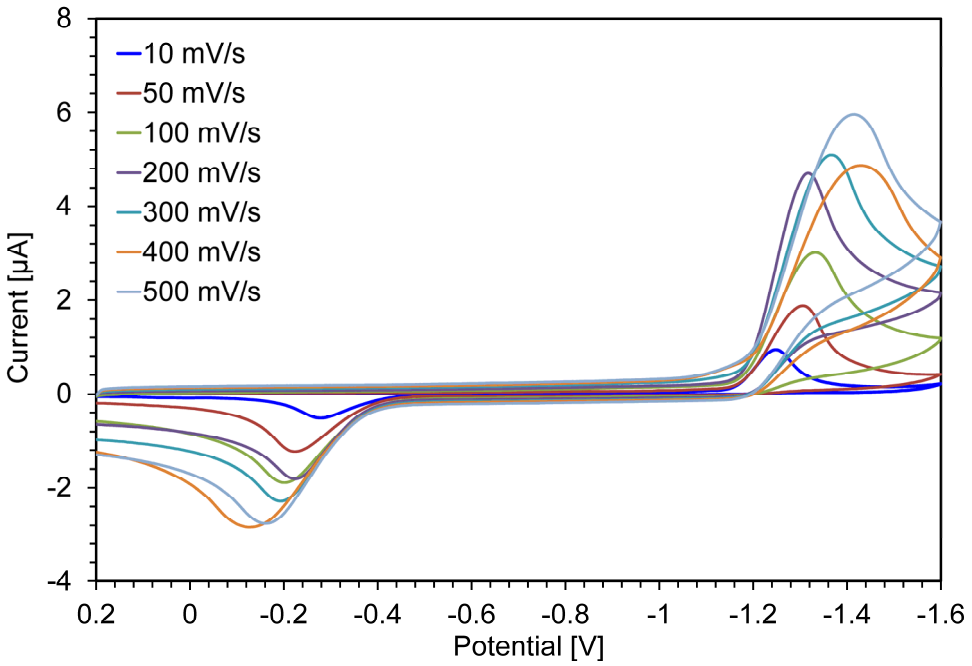

Figure 6. Cyclic voltammograms for the reduction of **22** in benzonitrile (1 mM) containing Et_4NClO_4 (0.1 M) as the supporting electrolyte at different scan rates.

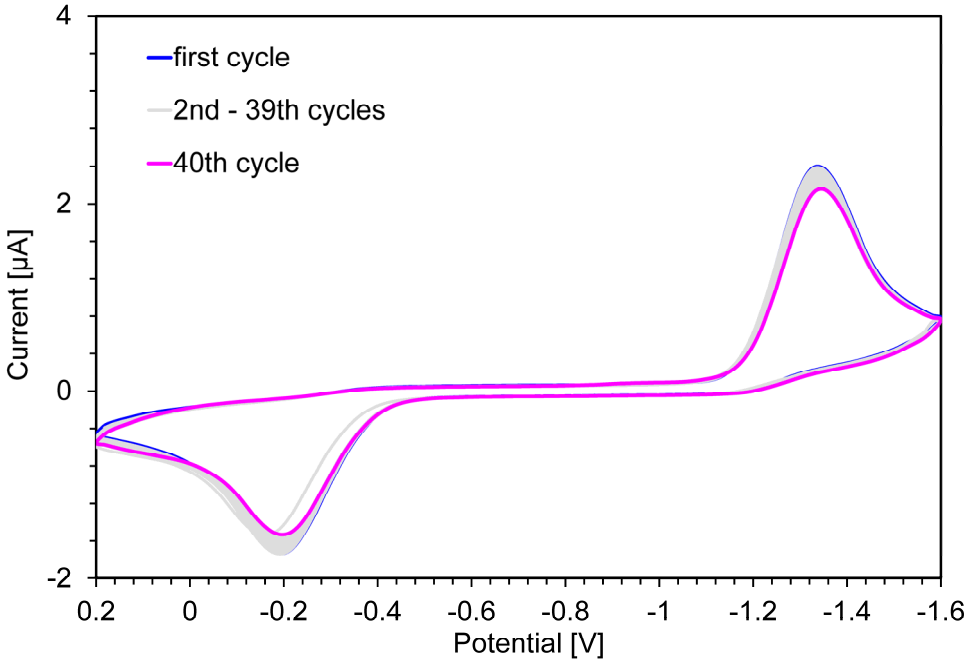

Figure 7. Cyclic voltammograms for the reduction of **22** in benzonitrile (1 mM) containing Et_4NClO_4 (0.1 M) as the supporting electrolyte during the 40 times continuous

measurements; scan rate = 100 mVs^{-1}.

To elucidate the electrochromic behavior of a series of benz[*a*]azulenes, the spectral changes were monitored by visible spectroscopy under the constant voltage redox conditions. As expected by the voltammetry experiments, most of the derivatives did not show reversible spectral changes under the redox conditions with the exception of some compounds. Despite the good reversibility seen in CV under the electrochemical oxidations, spectroelectrochemical measurements did not yield reversible electrochromism at **15**, **18a**, and **18b**. These results imply that the radical cationic species produced by the electrochemical oxidation of **15**, **18a**, and **18b** are not stable enough to be observed by the spectroelectrochemical measurements.

Spectroelectrochemical measurements of **9** and **22** under the reduction conditions showed relatively good reversible electrochromic behavior, even though the CV measurements did not show complete reversibility. For example, electrochemical reduction of **9** developed a new absorption band at around 420 nm along with the disappearance of the original band at ca. 455 nm. The reverse oxidation of the reduced species of **9** decreased the newly generated absorption bands, and the original spectrum was recovered with a relatively good reversibility (74% recovery). Similarly, electrochemical reduction of **22** with a dicyanovinyl group produced a new absorption band at around 460 nm together with a decrease in the original absorption band at 510 nm (Figure 8, top). The reverse oxidation of the reduced species of **22** regenerated the parent spectrum with a high recovery of 83% (Figure 8, bottom). Given the comprehensive results of CV and spectroelectrochemical measurements, the reversibility of **22** in the electrochromism may be explained by the subsequent reaction of the reduced species to produce another stable species. That is, the cathodic peak potential (E_{pc}) of **22** detected at −1.33 V in CV could be ascribed to the generation of radical anion, which is transformed into a more stable chemical species. The

reverse peak for the anodic process (E_{pa}) of **22** could be considered as the regeneration of the original neutral species from the newly generated species in the cathodic process, but it was not perfect.

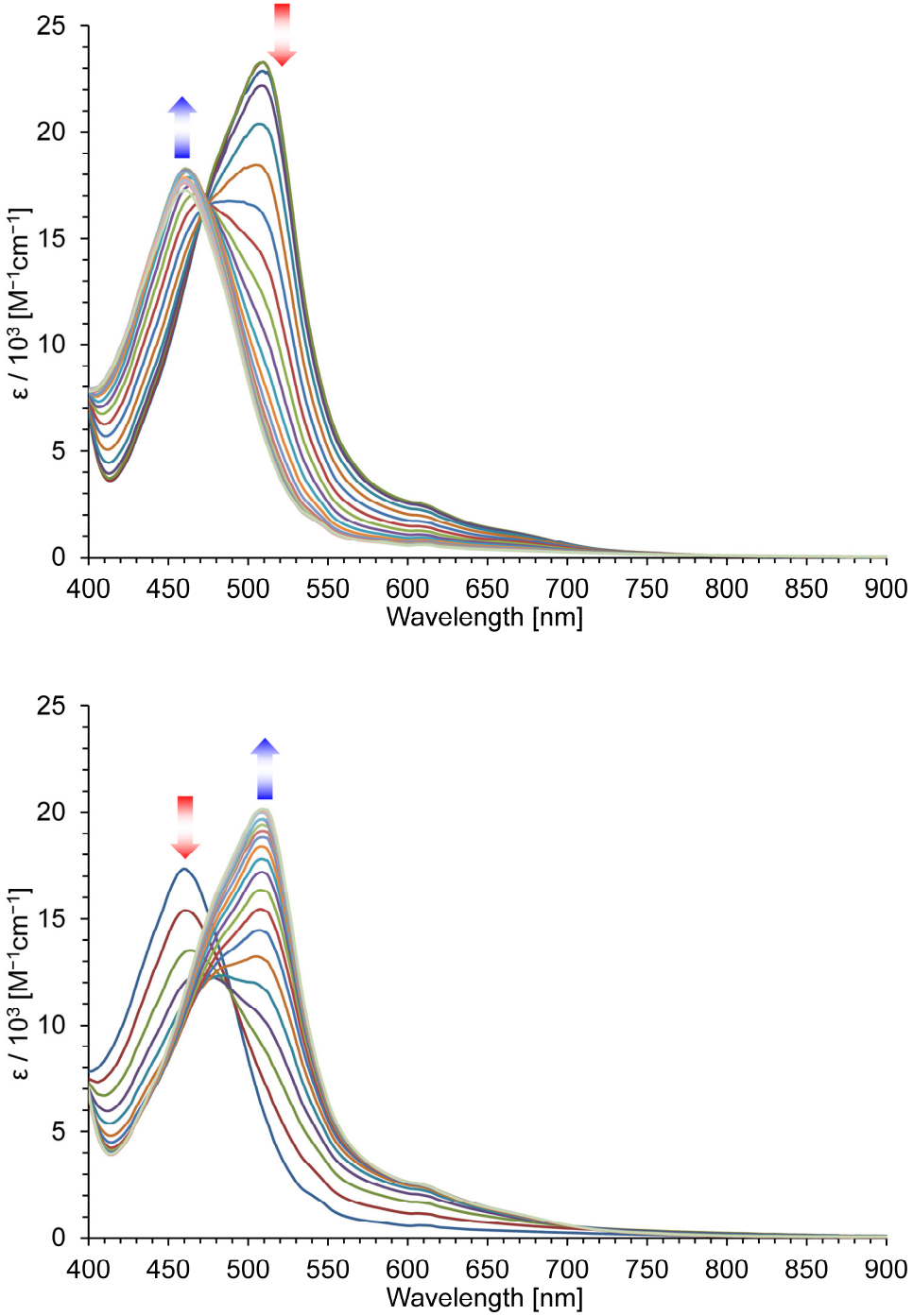

Figure 8. Continuous change in the visible spectrum of **22**: constant voltage electrochemical reduction at −1.60 V (top) and reverse oxidation of the reduced species at ±0 V (bottom) in benzonitrile containing Et_4NClO_4 (0.1 M) at 30 sec intervals.

The redox cycle of **25** also revealed good reversibility under the spectroelectrochemical measurement conditions. Electrochemical reduction of **25** at −1.60 V resulted in the disappearance of the absorption bands between 450–700 nm with an isosbestic point at λ = 445 nm accompanied by the appearance of a new band at 500 nm (Figure 9, top). The reverse oxidation of the reduced species for **25** regenerated the original absorption band with a recovery ratio of 73% (Figure 9, bottom). As with **9** and **22**, the cyclohexenone moiety serves as an electron-withdrawing group, so the reversibility of **25** might also be derived from the formation of stable anionic species, followed by the reactions under the electrochemical reduction conditions.

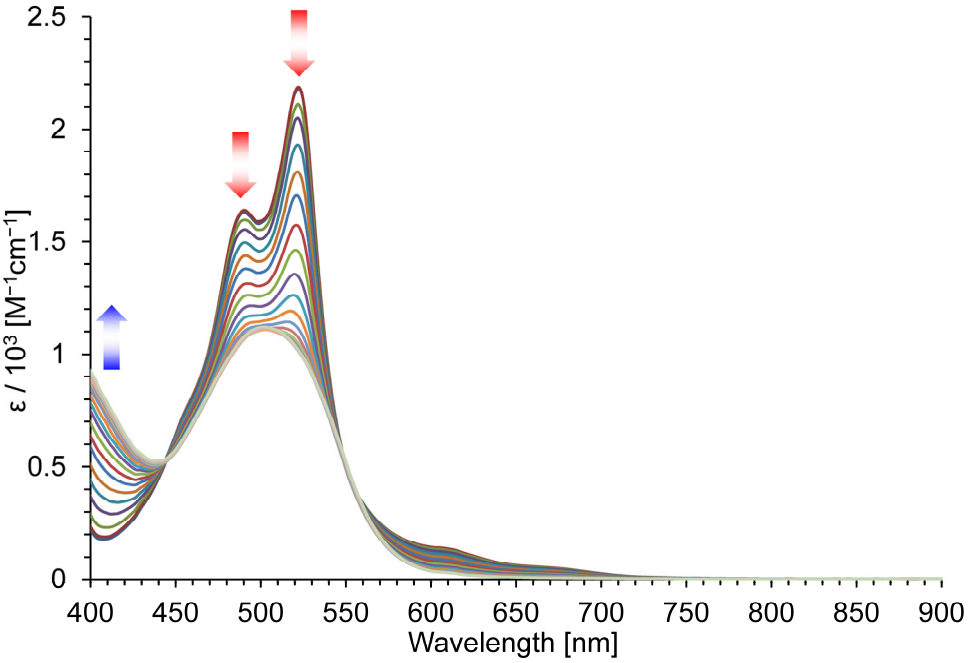

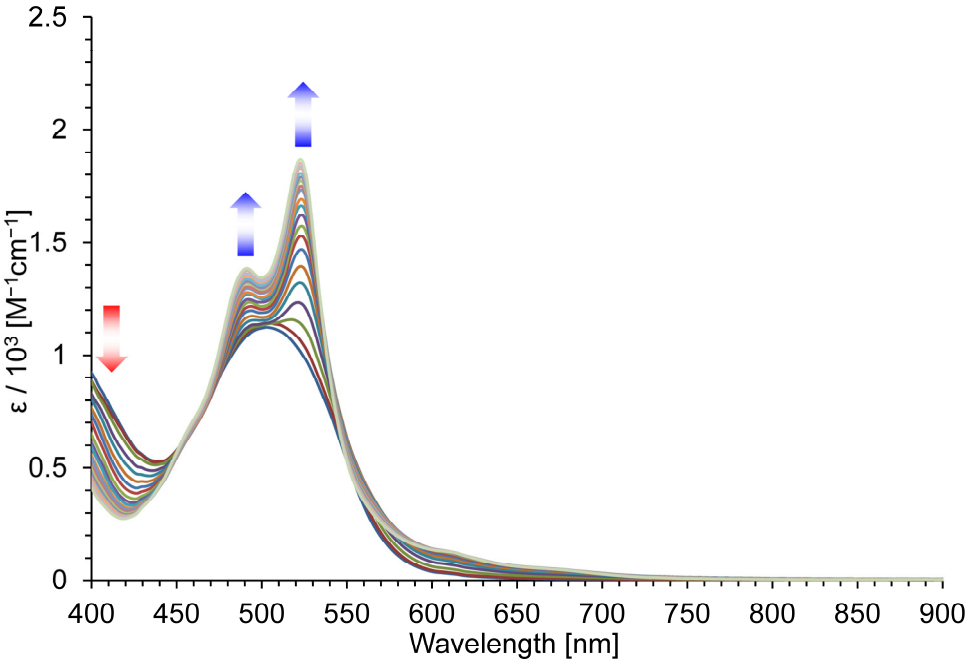

Figure 9. Continuous change in the visible spectrum of **25**: constant voltage electrochemical reduction at −1.60 V (top) and reverse oxidation of the reduced species at ±0 V (bottom) in benzonitrile containing Et_4NClO_4 (0.1 M) at 30 sec intervals.

Conclusion

In conclusion, we have described a new procedure for the synthesis of benz[*a*]azulenes from readily available 2*H*-cyclohepta[*b*]furan-2-one derivatives. This method should provide a new synthetic pathway for benz[*a*]azulenes, which are difficult and/or laborious to prepare by traditional methods. In this method, the azulene ring was constructed by [8 + 2] cycloaddition of 2*H*-cyclohepta[*b*]furan-2-ones with enamines prepared by the reaction of 4-*tert*-butylcyclohexanone with pyrrolidine. The resulting azulene derivatives were subsequently transformed into benz[*a*]azulenes *via* the Vilsmeier reaction, followed by the deformylation and elimination of the *tert*-butyl group with 100% H_3PO_4, and the final aromatization with DDQ. This four-step method of **5a** provided the highest yield among the methods reported so far. The formyl derivative **6a** was also transformed to cyclohept[*a*]acenaphthylen-3-one derivative **25** by Knoevenagel condensation with dimethyl

malonate, followed by intramolecular cyclization with Brønsted acid.

The decrease in aromaticity of the azulene moiety in benz[*a*]azulenes was suggested by the results of ^{1}H NMR spectra, NICS calculations, and single-crystal X-ray structure analysis. The optical and electrochemical properties of the parent benz[*a*]azulene and their functionalized derivatives were evaluated by UV/Vis and fluorescence measurements, voltammetry experiments, and spectroelectrochemistry, which revealed that the substituents on the azulene ring directly affected their properties. As previously reported, benz[*a*]azulenes did not show the strong emission in neutral media, but under acidic conditions, protonation of azulenes at the five-membered ring led to the formation of an azulenium ion, providing the remarkable fluorescence.

Most of benz[*a*]azulenes did not show reversible redox waves on CV, but those with electron-withdrawing groups showed a remarkable spectral change under the electrochemical reduction conditions. Furthermore, the reverse oxidation of these species regenerated the parent spectrum with a high recovery, which may be explained by the stability of the generated species.

As noted in the Introduction section, the construction of novel polycyclic aromatic compounds is expected for the application to the promising organic electronic materials. Hence, further functionalization and extension of the conjugated system of benz[*a*]azulenes may lead to the optical and electrochemical properties required for practical electronic materials. The preparation of novel π-electron systems based on benz[*a*]azulene frameworks and the elucidation of their properties are currently underway in our laboratory.

EXPERIMENTAL SECTION

General Methods: ^{1}H and ^{13}C NMR spectra were measured at 500 MHz (^{1}H NMR) and 125 MHz (^{13}C NMR), respectively. The fluorescence quantum yield was obtained with an absolute photoluminescence quantum yield spectrometer. The fluorescence lifetimes were

obtained with a time-resolved fluorescence spectrometer based on a streak camera. The time resolution was about 500 ps. The excitation wavelength was 400 nm (second harmonic of the output from a Ti: sapphire laser). The repetition rate of the oscillator was reduced from 80 to 8 MHz with a pulse selector. Voltammetry measurements were carried out in benzonitrile as a measurement solvent, with Pt working and auxiliary electrodes and a reference electrode formed from $Ag/AgNO_3$ (0.01 M) in acetonitrile containing tetrabutylammonium perchlorate (0.1 M).

Compound 2a: To a solution of **1a** (1.49 g, 10.2 mmol) in EtOH (30 mL) was added pyrrolidine enamine of 4-*tert*-butylcyclohexanone (8.29 g, 40.0 mmol). The resulting mixture was refluxed for 6 h. The solvent was removed under reduced pressure and the residue was purified by column chromatography on alumina with hexane as an eluent to give **2a** (2.06 g, 85%) as a blue solid. M.p. 42–43 °C; IR (AT-IR): ν_{max} = 2959 (w), 2910 (w), 1572 (w), 1537 (w), 1493 (w), 1453 (w), 1425 (w), 1389 (m), 1365 (m), 1318 (w), 1298 (w), 1242 (w), 941 (w), 830 (w), 797 (m), 787 (s), 765 (w), 739 (m), 729 (s), 708 (w), 671 (w), 659 (w) cm^{-1}; ^1H NMR (500 MHz, $CDCl_3$): δ_H = 8.14 (m, 2H, 5-H, 9-H), 7.46 (t, *J* = 9.7 Hz, 1H, 7-H), 7.13 (s, 1H, 10-H), 7.02–7.10 (m, 2H, 6-H, 8-H), 3.22–3.31 (m, 2H, *c*-Hex), 3.01–3.07 (m, 1H, *c*-Hex), 2.74 (m, 1H, *c*-Hex), 2.14–2.18 (m, 1H, *c*-Hex), 1.62 (m, 1H, *c*-Hex), 1.49–1.56 (m, 1H, *c*-Hex), 1.05 (s, 9H, *t*-Bu) ppm; ^{13}C NMR (125 MHz, $CDCl_3$): δ_C = 150.5, 140.2, 136.2, 135.5, 134.3, 130.9, 126.7, 122.2, 121.5, 114.8, 45.6, 32.9, 27.71, 27.65, 25.3, 24.5 ppm; HRMS (MALDI–TOF, positive) calcd for $C_{18}H_{22}^+$ $[M]^+$ 238.1716, found 238.1729.

Compound 2b: To a solution of **1b** (5.64 g, 30.0 mmol) in EtOH (90 mL) was added pyrrolidine enamine of 4-*tert*-butylcyclohexanone (20.7 g, 99.8 mmol). The resulting mixture was refluxed for 22.5 h. The solvent was removed under reduced pressure and the residue was purified by column chromatography on alumina with hexane as an eluent to give **2b**

(5.76 g, 68%) as a blue solid. M.p. 70–72 °C; IR (AT-IR): ν_{max} = 2957 (s), 2912 (m), 1574 (w), 1520 (w), 1490 (w), 1465 (m), 1445 (w), 1395 (m), 1363 (s), 1329 (w), 1302 (w), 1265 (w), 1242 (w), 1189 (w), 1088 (w), 1033 (w), 978 (w), 936 (w), 916 (w), 879 (w), 833 (w), 780 (s), 713 (w), 702 (w), 681 (w), 661 (w) cm^{-1}; ^1H NMR (500 MHz, $CDCl_3$): δ_H = 8.12 (s, 1H, 9-H), 8.02 (d, *J* = 9.8 Hz, 1H, 5-H), 7.41 (d, *J* = 9.8 Hz, 1H, 7-H), 7.26 (s, 1H, 10-H), 7.05 (t, *J* = 9.8 Hz, 1H, 6-H), 3.19–3.26 (m, 2H, *c*-Hex), 3.02–3.06 (m, 2H, *i*-Pr, *c*-Hex), 2.69 (m, 1H, *c*-Hex), 2.14 (m, 1H, *c*-Hex), 1.60–1.61 (m, 1H, *c*-Hex), 1.48 (m, 1H, *c*-Hex), 1.35 (d, *J* = 6.9 Hz, 6H, *i*-Pr), 1.04 (s, 9H, *t*-Bu) ppm; ^{13}C NMR (125 MHz, $CDCl_3$): δ_C = 150.5, 142.1, 140.3, 135.8, 134.5, 133.9, 129.6, 125.7, 121.3, 113.3, 45.7, 38.6, 32.9, 27.69, 27.65, 25.4, 24.7, 24.4 ppm; HRMS (MALDI–TOF, positive) calcd for $C_{21}H_{28}^+$ $[M]^+$ 280.2186, found 280.2204.

Compound 2c: To a solution of **1c** (941 mg, 5.00 mmol) in EtOH (15 mL) was added pyrrolidine enamine of 4-*tert*-butylcyclohexanone (4.15 g, 20.0 mmol). The resulting mixture was refluxed for 3.5 h and the solvent was removed under reduced pressure. The crude product was purified by column chromatography on alumina with hexane as an eluent to give **2c** (610 mg, 44%) as blue oil. IR (AT-IR): ν_{max} = 2959 (s), 2869 (w), 1698 (w), 1578 (s), 1548 (w), 1496 (w), 1464 (w), 1397 (m), 1364 (s), 1326 (w), 1274 (w), 1239 (w), 1173 (w), 1093 (w), 1041 (m), 957 (w), 908 (w), 836 (s), 779 (w), 759 (s), 733 (w), 705 (w), 668 (m) cm^{-1}; ^1H NMR (500 MHz, $CDCl_3$): δ_H = 8.06 (m, 2H, 5-H, 9-H), 7.02–6.97 (m, 3H, 6-H, 8-H, 10-H), 3.17–3.26 (m, 2H, *c*-Hex), 2.97–3.04 (m, 2H, *i*-Pr, *c*-Hex), 2.69 (m, 1H, *c*-Hex), 2.11–2.15 (m, 1H, *c*-Hex), 1.44–1.63 (m, 2H, *c*-Hex), 1.33 (d, *J* = 6.9 Hz, 6H, *i*-Pr), 1.03 (s, 9H, *t*-Bu) ppm; ^{13}C NMR (125 MHz, $CDCl_3$): δ_C = 157.2, 149.0, 138.9, 134.9, 134.0, 130.7, 126.5, 121.4, 120.5, 114.4, 45.7, 39.7, 32.9, 27.65, 27.57, 25.4, 24.5, 24.4 ppm; HRMS (MALDI–TOF, positive) calcd. for $C_{21}H_{28}^+$ $[M]^+$ 280.2186, found 280.2182.

Compound 3a: $POCl_3$ (330 mg, 2.15 mmol) was added at 0 °C to a solution of **2a** (155 mg,

0.582 mmol) in DMF (20 mL). The resulting mixture was stirred at room temperature for 2 h. The reaction mixture was poured into K_2CO_3 aq., extracted with toluene, washed with brine, and dried with Na_2SO_4. The crude product was purified by column chromatography on silica gel with AcOEt as an eluent to give **3a** (134 mg, 86%) as a purple solid. M.p. 79–80 °C; IR (AT-IR): ν_{max} = 2956 (w), 2868 (w), 1638 (s), 1592 (w), 1536 (w), 1521 (w), 1438 (s), 1407 (m), 1394 (m), 1380 (m), 1363 (s), 1295 (w), 1244 (w), 1227 (w), 1175 (w), 1118 (w), 1031 (w), 998 (w), 979 (w), 942 (w), 896 (w), 845 (w), 785 (w), 737 (s), 702 (w), 676 (w) cm^{-1}; ^1H NMR (500 MHz, $CDCl_3$): δ_H = 10.45 (s, 1H, CHO), 9.27 (d, *J* = 9.7 Hz, 1H, 9-H), 8.22 (d, *J* = 9.7 Hz, 1H, 5-H), 7.68 (t, *J* = 9.7 Hz, 1H, 7-H), 7.48 (t, *J* = 9.7 Hz, 1H, 8-H), 7.42 (t, *J* = 9.7 Hz, 1H, 6-H), 3.58 (m, 1H, *c*-Hex), 3.09–3.12 (m, 2H, *c*-Hex), 2.55–2.60 (m, 1H, *c*-Hex), 2.21–2.17 (m, 1H, *c*-Hex), 1.54–1.57 (m, 1H, *c*-Hex), 1.46–1.40 (m, 1H, c-Hex), 1.03 (s, 9H, *t*-Bu) ppm; ^{13}C NMR (125 MHz, $CDCl_3$): δ_C = 185.0, 154.6, 142.7, 141.2, 137.8, 134.6, 133.2, 129.2, 128.3, 127.5, 120.5, 44.9, 32.7, 27.5, 26.4, 24.6, 24.0 ppm; HRMS (MALDI–TOF, positive) calcd for $C_{19}H_{22}O + H^+$ $[M + H]^+$ 267.1743, found 267.1735; HRMS (MALDI–TOF, positive) calcd for $C_{19}H_{22}O + Ag^+$ $[M + Ag]^+$ 373.0716, found 373.0735.

Compound 3b: $POCl_3$ (5.91 g, 38.5 mmol) was added at 0 °C to a solution of **2b** (3.54 g, 12.6 mmol) in DMF (40 mL). The resulting mixture was stirred at room temperature for 30 min. The reaction mixture was poured into K_2CO_3 aq., extracted with hexane/AcOEt, washed with brine, and dried with Na_2SO_4. The crude product was purified by column chromatography on silica gel with hexane/AcOEt (1:1) as an eluent to give **3b** (3.86 g, 99%) as a purple solid. M.p. 99–101 °C; IR (AT-IR): ν_{max} = 2957 (m), 2902 (w), 1632 (s), 1599 (w), 1530 (w), 1465 (m), 1441 (s), 1402 (w), 1375 (s), 1362 (m), 1329 (w), 1301 (w), 1227 (w), 1176 (w), 1001 (w), 978 (w), 956 (w), 942 (w), 802 (m), 727 (w), 668 (w) cm^{-1}; ^1H NMR (500 MHz, $CDCl_3$) δ_H = 10.42 (s, 1H, CHO), 9.42 (s, 1H, 9-H), 8.15 (d, *J* = 10.0 Hz, 1H, 5-H), 7.67 (d, *J* = 10.0 Hz, 1H, 7-H), 7.43 (t, *J* = 10.0 Hz, 1H, 6-H), 3.61–3.57 (m, 1H, *c*-Hex), 3.20

(sept., *J* = 6.9 Hz, 1H, *i*-Pr), 3.07–3.14 (m, 2H, *c*-Hex), 2.61–2.56 (m, 1H, *c*-Hex), 2.18–2.22 (m, 1H, *c*-Hex), 1.56–1.61 (m, 1H, *c*-Hex), 1.47 (m, 1H, *c*-Hex), 1.40 (d, *J* = 6.9 Hz, 6H, *i*-Pr), 1.04 (s, 9H, *t*-Bu) ppm; ^{13}C NMR (125 MHz, $CDCl_3$): δ_C = 184.4, 154.9, 151.2, 142.8, 141.7, 136.5, 135.2, 131.7, 127.7, 127.4, 119.7, 45.1, 39.2, 32.8, 27.6, 26.2, 24.74, 24.66, 24.0 ppm; HRMS (MALDI–TOF, positive) calcd for $C_{22}H_{28}O + H^+$ $[M + H]^+$ 309.2213, found 309.2219, HRMS (MALDI–TOF, positive) calcd for $C_{22}H_{28}O + Ag^+$ $[M + Ag]^+$ 415.1186, found 415.1172.

Compound 3c: $POCl_3$ (335 mg, 2.18 mmol) was added at 0 °C to a solution of **2c** (201 mg, 0.717 mmol) in DMF (30 mL). The resulting mixture was stirred at room temperature for 16.5 h. The reaction mixture was poured into K_2CO_3 aq., extracted with toluene, washed with brine, and dried with Na_2SO_4. The crude product was purified by column chromatography on silica gel with AcOEt as an eluent to give **3c** (204 mg, 92%) as red oil. IR (AT-IR): ν_{max} = 2960 (w), 1637 (s), 1581 (m), 1441 (m), 1401 (m), 1379 (m), 1364 (m), 1304 (w), 1240 (w), 1046 (w), 997 (w), 975 (w), 957 (w), 923 (w), 840 (m), 754 (s), 675 (m), 664 (m) cm^{-1}; ^{1}H NMR (500 MHz, $CDCl_3$): δ_H = 10.44 (s, 1H, CHO), 9.23 (d, *J* = 10.3 Hz, 1H, 9-H), 8.20 (d, *J* = 10.3 Hz, 1H, 5-H), 7.45 (dd, *J* = 10.3, 1.2 Hz, 1H, 8-H), 7.39 (dd, *J* = 10.3, 1.2 Hz, 1H, 6-H), 3.61–3.56 (m, 1H, *c*-Hex), 3.15–3.07 (m, 3H, *i*-Pr, *c*-Hex), 2.62–2.56 (m, 1H, *c*-Hex), 2.21–2.17 (m, 1H, *c*-Hex), 1.62–1.56 (m, 1H, *c*-Hex), 1.51–1.42 (m, 1H, *c*-Hex), 1.36 (d, *J* = 6.9 Hz, 6H, *i*-Pr), 1.03 (s, 9H, *t*-Bu) ppm; ^{13}C NMR (125 MHz, $CDCl_3$): δ_C = 185.0, 160.2, 153.2, 141.5, 140.1, 134.5, 133.0, 128.4, 128.0, 127.0, 120.5, 45.1, 39.7, 32.8, 27.6, 26.3, 24.8, 24.4, 24.0 ppm; HRMS (MALDI–TOF, positive) calcd for $C_{22}H_{28}O + H^+$ $[M + H]^+$ 309.2213, found 309.2241.

Compound 4a: DDQ (337 mg, 1.48 mmol) was added at 0 °C to a solution of **3a** (134 mg, 0.503 mmol) in toluene (15 mL). The resulting mixture was stirred at room temperature for 2

h. The reaction mixture was poured into K_2CO_3 aq., extracted with toluene/EtOAc, washed with brine, and dried with Na_2SO_4. The crude product was purified by column chromatography on silica gel with toluene/AcOEt (4:1) as an eluent to give **4a** (130 mg, 99%) as a green solid. M.p. 125–126 °C; IR (AT-IR): ν_{max} = 2970 (w), 2954 (w), 1635 (s), 1607 (w), 1491 (w), 1468 (m), 1449 (w), 1410 (w), 1391 (m), 1365 (m), 1329 (w), 1293 (w), 1274 (w), 1244 (w), 1212 (w), 1187 (w), 1153 (w), 1094 (w), 1076 (w), 1031 (w), 1018 (w), 992 (w), 939 (w), 876 (w), 861 (w), 841 (w), 825 (m), 776 (w), 766 (w), 741 (w), 709 (s), 655 (w) cm^{-1}; UV/Vis (CH_2Cl_2): λ_{max} (log ε) = 240 (4.36), 284 (4.52), 337 (4.44), 350 (4.52), 391 sh (3.73), 412 (3.85), 434 (3.93), 541 (2.69), 587 (2.67), 643 sh (2.53), 716 sh (2.28) nm; UV/Vis (10% TFA/CH_2Cl_2): λ_{max} (log ε) = 307 (4.50), 293 sh (4.45), 372 (4.25), 431 (3.96) nm; ^{1}H NMR (500 MHz, $CDCl_3$): δ_H = 10.81 (s, 1H, CHO), 9.24 (d, *J* = 10.6 Hz, 1H, 9-H), 8.84 (dd, *J* = 8.9, 0.9 Hz, 1H, 5-H), 8.57 (d, *J* = 8.6 Hz, 1H, 1-H), 8.41 (d, *J* = 1.4 Hz, 1H, 4-H), 7.91 (dd, *J* = 8.6, 1.4 Hz, 1H, 2-H), 7.73–7.69 (m, 1H, 7-H), 7.58 (dd, *J* = 10.6, 9.3 Hz, 1H, 8-H), 7.53 (dd, *J* = 10.7, 8.9 Hz, 1H, 6-H), 1.50 (s, 9H, *t*-Bu) ppm; ^{13}C NMR (125 MHz, $CDCl_3$): δ_C = 184.8, 147.1, 145.9, 143.0, 139.1, 138.1, 134.5, 132.7, 130.7, 130.6, 130.0, 129.3, 120.4, 119.5, 116.7, 35.3, 31.8 ppm; HRMS (MALDI–TOF, positive) calcd for $C_{19}H_{18}O + H^+$ $[M + H]^+$ 263.1430, found 263.1418, HRMS (MALDI–TOF, positive) calcd for $C_{19}H_{18}O + Ag^+$ $[M + Ag]^+$ 369.0403, found 369.0417.

Compound 4b: DDQ (1.02 g, 4.48 mmol) was added at 0 °C to a solution of **3b** (454 mg, 1.47 mmol) in toluene (30 mL). The resulting mixture was stirred at room temperature for 1.5 h. The reaction mixture was poured into K_2CO_3 aq., extracted with toluene/EtOAc, washed with brine, and dried with Na_2SO_4. The crude product was purified by column chromatography on silica gel with toluene/EtOAc (4:1) as an eluent to give **4b** (443 mg, 99%) as a green solid. M.p. 119–121 °C; IR (AT-IR): ν_{max} = 2959 (m), 2867 (w), 1636 (s), 1618 (m), 1509 (w), 1475 (s), 1416 (m), 1386 (m), 1368 (s), 1306 (w), 1276 (w), 1254 (w),

1219 (w), 1191 (m), 1152 (w), 1069 (w), 1038 (m), 1002 (w), 954 (w), 930 (w), 894 (w), 870 (w), 840 (w), 827 (w), 796 (s), 776 (w), 734 (w), 707 (w), 656 (w) cm^{-1}; UV/Vis (CH_2Cl_2): λ_{max} (log ε) = 243 (4.37), 287 (4.56), 339 (4.47), 352 (4.55), 414 sh (3.90), 434 (3.99), 540 (2.81), 586 (2.82), 644 sh (2.69) nm; UV/Vis (10% TFA/CH_2Cl_2): λ_{max} (log ε) = 262 (4.44), 292 sh (4.44), 371 (4.28), 390 (4.21), 430 sh (3.96) nm; ^{1}H NMR (500 MHz, $CDCl_3$): δ_H = 10.81 (s, 1H, CHO), 9.30 (s, 1H, 9-H), 8.75 (d, *J* = 8.9 Hz, 1H, 5-H), 8.52 (d, *J* = 8.6 Hz, 1H, 1-H), 8.36 (d, *J* = 1.5 Hz, 1H, 4-H), 7.86 (dd, *J* = 8.6, 1.5 Hz, 1H, 2-H), 7.67 (d, *J* = 11.2 Hz, 1H, 7-H), 7.54 (dd, *J* = 11.2, 8.9 Hz, 1H, 6-H), 3.20 (sept, *J* = 6.9 Hz, 1H, *i*-Pr), 1.48 (s, 9H, *t*-Bu), 1.42 (d, *J* = 6.9 Hz, 6H, *i*-Pr) ppm; ^{13}C NMR (125 MHz, $CDCl_3$): δ_C = 184.4, 152.3, 146.6, 145.9, 143.1, 139.5, 138.6, 132.6, 131.8, 130.3, 129.7, 129.1, 120.0, 118.6, 116.7, 39.5, 35.2, 31.8, 24.3 ppm; HRMS (MALDI–TOF, positive) calcd for $C_{22}H_{24}O + H^+$ $[M + H]^+$ 305.1900, found 305.1914.

Compound 4c: DDQ (468 mg, 2.06 mmol) was added at 0 °C to a solution of **3c** (308 mg, 1.00 mmol) in toluene (15 mL). The resulting mixture was stirred at room temperature for 1 h. The reaction mixture was poured into K_2CO_3 aq. and extracted with toluene. The organic layer was washed with brine and dried with Na_2SO_4. The crude product was purified by column chromatography on silica gel with toluene/EtOAc (2:1) as an eluent to give **4c** (289 mg, 95%) as a green solid. M.p. 104 °C; IR (AT-IR): ν_{max} = 2966 (w), 2875 (w), 1628 (s), 1604 (m), 1585 (m), 1525 (w), 1490 (w), 1458 (s), 1419 (m), 1404 (m), 1369 (s), 1333 (w), 1283 (w), 1265 (w), 1244 (w), 1231 (w), 1220 (m), 1196 (w), 1154 (w), 1132 (w), 1084 (w), 1052 (w), 1033 (m), 976 (m), 924 (w), 908 (w), 870 (w), 857 (w), 843 (m), 828 (m), 780 (w), 719 (m), 653 (m) cm^{-1}; UV/Vis (CH_2Cl_2): λ_{max} (log ε) = 243 (4.36), 286 (4.51), 341 (4.44), 354 (4.53), 410 sh (3.83), 436 (3.95), 528 (2.86), 563 (2.85), 623 sh (2.68) nm; UV/Vis (10% TFA/CH_2Cl_2): λ_{max} (log ε) = 261 (4.27), 290 sh (4.38), 308 (4.48), 371 (4.28), 395 sh (4.18), 450 sh (3.86) nm; ^{1}H NMR (500 MHz, $CDCl_3$): δ_H = 10.81 (s, 1H, CHO), 9.21 (d, *J* = 11.5 Hz,

1H, 9-H), 8.78 (d, *J* = 9.5 Hz, 1H, 5-H), 8.54 (d, *J* = 8.5 Hz, 1H, 1-H), 8.37 (d, *J* = 1.7 Hz, 1H, 4-H), 7.86 (dd, *J* = 8.5, 1.7 Hz, 1H, 2-H), 7.48–7.50 (m, 2H, 6-H, 8-H), 3.14 (sept, *J* = 6.9 Hz, 1H, *i*-Pr), 1.49 (s, 9H, *t*-Bu), 1.39 (d, *J* = 6.9 Hz, 6H, *i*-Pr) ppm; ^{13}C NMR (125 MHz, $CDCl_3$): δ_C = 185.0, 160.5, 146.7, 145.0, 140.9, 138.8, 134.2, 132.7, 131.5, 130.7, 128.6, 127.4, 120.3, 119.2, 116.4, 39.6, 35.2, 31.8, 24.1 ppm; HRMS (MALDI–TOF, positive) calcd for $C_{22}H_{24}O + H^+$ $[M + H]^+$ 305.1900, found 305.1881.

Compound 5a: A solution of **4a** (394 mg, 1.50 mmol) in 100% H_3PO_4 (35 mL) was stirred at 140 °C for 19 h. After cooling to room temperature, the reaction mixture was poured into water, and neutralized with KOH aq. The precipitate was collected by filtration and dissolved in $CHCl_3$. The crude product was purified by silica gel column chromatography with hexane/toluene (10:1) as an eluent to give **5a** (190 mg, 71%) as green crystals. M.p. 150 °C; IR (AT-IR): ν_{max} = 3046 (w), 1698 (w), 1601 (m), 1586 (w), 1558 (w), 1523 (w), 1448 (w), 1433 (w), 1397 (w), 1377 (w), 1324 (w), 1308 (w), 1264 (w), 1240 (w), 1206 (w), 1159 (w), 1046 (w), 1012 (w), 975 (w), 934 (w), 910 (w), 885 (w), 870 (w), 855 (w), 811 (m), 763 (m), 740 (m), 682 (s), 653 (w) cm^{-1}; UV/Vis (CH_2Cl_2): λ_{max} (log ε) = 247 (4.03), 256 sh (4.00), 306 (4.68), 320 sh (4.39), 345 (3.47), 363 (3.60), 381 (3.65), 402 (3.47), 475 sh (2.54), 517 sh (2.61), 561 (2.69), 612 (2.70), 673 (2.60), 764 sh (2.41) nm; UV/Vis (10% TFA/CH_2Cl_2): λ_{max} (log ε) = 274 (4.32), 398 (4.37) nm; ^{1}H NMR (500 MHz, $CDCl_3$): δ_H = 8.39 (dd, *J* = 8.0, 0.9 Hz, 4-H), 8.32 (dd, *J* = 8.3, 0.6 Hz, 1H, 5-H), 7.96 (d, *J* = 11.0 Hz, 1H, 9-H), 7.87 (d, *J* = 8.0 Hz, 1H, 1-H), 7.69–7.66 (m, 1H, 2-H), 7.50–7.47 (m, 1H, 3-H), 7.33 (s, 1H, 10-H), 7.20 (dd, *J* = 11.0, 8.3 Hz, 1H, 7-H), 7.04 (dd, *J* = 11.0, 8.3 Hz, 1H, 8-H), 6.85 (dd, *J* = 10.9, 8.6 Hz, 1H, 6-H) ppm; ^{13}C NMR (125 MHz, $CDCl_3$): δ_C = 142.5, 140.7, 139.3, 136.1, 134.8, 131.5, 128.6, 128.0, 125.5, 123.8, 121.9, 120.9, 120.4, 116.2 ppm; HRMS (MALDI–TOF, positive) calcd for $C_{14}H_{10}^+$ $[M]^+$ 178.0777, found 178.0771.

Compound 5b: A solution of **4b** (549 mg, 1.80 mmol) in 100% H_3PO_4 (40 mL) was stirred at 140 °C for 14 h. After cooling to room temperature, the reaction mixture was poured into water and neutralized with KOH aq. The precipitate was collected by filtration and dissolved in $CHCl_3$. The crude product was purified by silica gel column chromatography with hexane as an eluent to give **5b** (194 mg, 49%) as green crystals. M.p. 140 °C; IR (AT-IR): ν_{max} = 2953 (w), 2928 (w), 2865 (w), 1601 (w), 1509 (w), 1464 (w), 1451 (w), 1430 (w), 1384 (w), 1362 (w), 1312 (w), 1248 (w), 1122 (w), 1065 (w), 1011 (w), 932 (w), 915 (w), 905 (w), 881 (w), 819 (s), 793 (m), 762 (s), 747 (m), 704 (s), 656 (w) cm^{-1}; UV/Vis (CH_2Cl_2): λ_{max} (log ε) = 248 (4.06), 306 (4.75), 346 (3.57), 362 (3.68), 380 (3.71), 401 (3.48), 519 sh (2.55), 568 (2.66), 616 (2.68), 679 (2.54), 774 sh (2.14) nm; UV/Vis (10% TFA/CH_2Cl_2): λ_{max} (log ε) = 275 (4.33), 397 (4.48) nm; ^{1}H NMR (500 MHz, $CDCl_3$): δ_H = 8.33 (d, *J* = 7.7 Hz, 1H, 4-H), 8.21 (dd, *J* = 8.2, 0.7 Hz, 1H, 5-H), 7.85 (s, 1H, 9-H), 7.81 (d, *J* = 7.7 Hz, 1H, 1-H), 7.64 (dd, *J* = 7.7, 1.0 Hz, 1H, 2-H), 7.42 (dd, *J* = 7.7, 1.0 Hz, 1H, 3-H), 7.21 (s, 1H, 10-H), 7.13 (d, *J* = 11.7 Hz, 1H, 7-H), 7.02 (dd, *J* = 11.7, 8.2 Hz, 1H, 6-H), 2.93 (sept, *J* = 6.9 Hz, 1H, *i*-Pr), 1.32 (d, *J* = 6.9 Hz, 6H, *i*-Pr) ppm; ^{13}C NMR (125 MHz, $CDCl_3$): δ_C = 143.2, 142.7, 140.8, 139.1, 135.8, 132.6, 131.4, 128.5, 127.2, 125.2, 121.4, 120.8, 120.0, 115.2, 38.4, 23.9 ppm; HRMS (MALDI–TOF, positive) calcd for $C_{17}H_{16}^+$ $[M]^+$ 220.1247, found 220.1226.

Compound 5c: A solution of **4c** (1.07 g, 3.50 mmol) in 100% H_3PO_4 (80 mL) was stirred at 140 °C for 15 h. After cooling to room temperature, the reaction mixture was poured into water and neutralized with KOH aq. The precipitate was collected by filtration and dissolved in $CHCl_3$. The crude product was purified by silica gel column chromatography with hexane as an eluent to give **5c** (316 mg, 41%) as green crystals. M.p. 127 °C ; IR (AT-IR): ν_{max} = 2958 (w), 2868 (w), 1601 (m), 1587 (w), 1524 (w), 1464 (w), 1442 (m), 1409 (m), 1213 (w), 1097 (w), 1074 (w), 1035 (w), 935 (w), 866 (w), 836 (s), 795 (w), 761 (s), 743 (s), 703 (m), 686 (w), 668 (w), 658 (m) cm^{-1}; UV/Vis (CH_2Cl_2): λ_{max} (log ε) = 245 (4.04), 301 sh (4.70), 309

(4.75), 324 (4.67), 346 (3.58), 363 (3.68), 383 (3.70), 402 (3.45), 501 (2.69), 548 (2.77), 592 (2.78), 660 sh (2.64), 732 sh (2.37) nm; UV/Vis (10% TFA/CH_2Cl_2): λ_{max} (log ε) = 274 (4.26), 397 (4.46) nm; ^{1}H NMR (500 MHz, $CDCl_3$): δ_H = 8.34 (d, *J* = 7.8 Hz, 1H, 1-H), 8.25 (d, *J* = 8.8 Hz, 1H, 5-H), 7.93 (d, *J* = 11.4 Hz, 1H, 9-H), 7.84 (d, *J* = 7.8 Hz, 1H, 4-H), 7.63–7.63 (m, 1H, 3-H), 7.45–7.42 (m, 1H, 2-H), 7.26 (s, 1H, 10-H), 6.95 (dd, *J* = 8.8, 1.3 Hz, 1H, 6-H), 6.81 (dd, *J* = 11.4, 1.3 Hz, 1H, 8-H), 2.93 (sept, *J* = 6.9 Hz, 1H, *i*-Pr), 1.31 (d, *J* = 6.9 Hz, 6H, *i*-Pr) ppm; ^{13}C NMR (125 MHz, $CDCl_3$): δ_C = 156.0, 142.2, 138.8, 138.6, 135.5, 131.8, 128.1, 125.0, 122.1, 121.7, 120.6, 120.4, 115.7, 39.4, 23.8 ppm; HRMS (MALDI–TOF, positive) calcd for $C_{17}H_{16}^+$ $[M]^+$ 220.1247, found 220.1228.

Compound 6a: A solution of **4a** (1.58 g, 6.03 mmol) in 100% H_3PO_4 (30 mL) was stirred at 140 °C for 3 h. After cooling to room temperature, the reaction mixture was poured into water, extracted with toluene, washed with NaOH aq. and brine, and dried with Na_2SO_4. The crude product was purified by silica gel column chromatography with $CHCl_3$/AcOEt (5:1) as an eluent to give **6a** (1.14 g, 92%) as a brown solid. M.p. 97 °C ; IR (AT-IR): ν_{max} = 1637 (s), 1604 (m), 1596 (m), 1556 (w), 1523 (m), 1475 (m), 1451 (m), 1424 (m), 1408 (w), 1395 (m), 1374 (m), 1340 (w), 1313 (w), 1263 (w), 1243 (w), 1201 (m), 1074 (m), 1026 (w), 956 (w), 938 (m), 871 (w), 860 (w), 767 (s), 705 (s), 670 (m), 660 (m) cm^{-1}; UV/Vis (CH_2Cl_2): λ_{max} (log ε) = 238 (4.38), 281 (4.50), 334 (4.45), 346 (4.51), 387 sh (3.73), 408 (3.88), 431 (3.97), 533 (2.78), 565 (2.76), 628 sh (2.62), 706 sh (2.25) nm; UV/Vis (10% TFA/CH_2Cl_2): λ_{max} (log ε) = 286 (4.40), 301 (4.44), 364 (4.34), 424 (4.05) nm; ^{1}H NMR (500 MHz, $CDCl_3$): δ_H = 10.76 (s, 1H, CHO), 9.13 (d, *J* = 10.9 Hz, 1H, 9-H), 8.66 (dd, *J* = 8.7, 1.0 Hz, 1H, 5-H), 8.58 (d, *J* = 8.0 Hz, 1H, 1-H), 8.31 (d, *J* = 8.0 Hz, 1H, 4-H), 7.77–7.74 (m, 1H, 2-H), 7.66–7.62 (m, 1H, 7-H), 7.54–7.43 (m, 3H, 3-H, 6-H, 8-H) ppm; ^{13}C NMR (125 MHz, $CDCl_3$): δ_C = 184.9, 145.6, 142.6, 140.9, 138.1, 134.3, 132.8, 130.9, 130.5, 130.1, 123.6, 121.0, 120.6, 119.5 ppm; HRMS (MALDI–TOF, positive) calcd for $C_{15}H_{10}O + H^+$ $[M + H]^+$ 207.0804, found 207.0809.

Synthesis of 6a by Vilsmeier reaction: $POCl_3$ (404 mg, 2.63 mmol) was added at 0 °C to a solution of **5a** (131 mg, 0.735 mmol) in DMF (30 mL). The resulting mixture was stirred at room temperature for 3 h. The reaction mixture was poured into K_2CO_3 aq. and extracted with toluene. The organic layer was washed with brine, dried with Na_2SO_4, and concentrated under reduced pressure. The crude product was purified by column chromatography on silica gel with $CHCl_3$/EtOAc (5:1) as an eluent to give **6a** (122 mg, 81%) as a brown solid.

Compound 6b: A solution of **4b** (779 mg, 2.56 mmol) in 100% H_3PO_4 (30 mL) was stirred at 140 °C for 3 h. After cooling to room temperature, the reaction mixture was poured into water, extracted with toluene, washed with brine, and dried with Na_2SO_4. The crude product was purified by silica gel column chromatography with $CHCl_3$/AcOEt (5:1) as an eluent to give **6b** (515 mg, 81%) as a greenish brown solid. M.p. 67–68 °C; IR (AT-IR): ν_{max} = 2967 (w), 1633 (s), 1615 (m), 1602 (m), 1508 (w), 1476 (m), 1425 (m), 1385 (m), 1367 (m), 1318 (w), 1293 (w), 1266 (w), 1251 (w), 1225 (w), 1210 (w), 1189 (w), 1152 (m), 1119 (w), 1087 (w), 1044 (m), 1016 (w), 941 (w), 905 (w), 861 (m), 807 (m), 767 (s), 753 (m), 719 (m), 710 (w), 685 (w) cm^{-1}; UV/Vis (CH_2Cl_2): λ_{max} (log ε) = 240 (4.37), 284 (4.52), 337 (4.45), 349 (4.52), 408 sh (3.89), 430 (3.99), 536 (2.85), 575 (2.83), 632 sh (2.68), 704 sh (2.39) nm; UV/Vis (10% TFA/CH_2Cl_2): λ_{max} (log ε) = 286 sh (4.50), 301 (4.54), 364 (4.43), 424 (4.14) nm; ^{1}H NMR (500 MHz, $CDCl_3$): δ_H = 10.83 (s, 1H, CHO), 9.30 (s, 1H, 9-H), 8.66 (d, *J* = 8.9 Hz, 1H, 5-H), 8.56 (d, *J* = 8.0 Hz, 1H, 1-H), 8.34 (dd, *J* = 8.0, 0.9 Hz, 1H, 4-H), 7.75 (t, *J* = 8.0 Hz, 1H, 2-H), 7.67 (d, *J* = 11.2 Hz, 1H, 7-H), 7.50–7.55 (m, 2H, 3-H, 6-H), 3.20 (sept, *J* = 6.9 Hz, 1H, *i*-Pr), 1.42 (d, *J* = 6.9 Hz, 6H, *i*-Pr) ppm; ^{13}C NMR (125 MHz, $CDCl_3$): δ_C = 184.7, 152.6, 145.6, 142.8, 141.5, 138.7, 132.5, 132.0, 130.4, 130.3, 129.9, 123.3, 121.0, 120.2, 118.8, 39.5, 24.3 ppm; HRMS (MALDI–TOF, positive) calcd for $C_{18}H_{16}O^+$ $[M]^+$ 248.1196, found 248.1215.

Compound 7: $NaBH_4$ (47 mg, 1.24 mmol) was added to a solution of **4c** (168 mg, 0.55 mmol) in THF (2 mL) and diglyme (0.5 mL), and the resulting mixture was stirred at room temperature for 1 h. Then, $NaBH_4$ (45 mg, 1.19 mmol) and $BF_3{\cdot}Et_2O$ (0.5 mL) was added to the reaction mixture and the solution was additionally stirred at the same temperature for 2 h. The reaction mixture was poured into water, extracted with hexane, washed with brine, and dried with Na_2SO_4. The crude product was purified by alumina column chromatography with hexane as an eluent to give **7** (31 mg, 19%) as green oil. IR (AT-IR): ν_{max} = 3567 (w), 2958 (s), 2869 (m), 2360 (m), 2342 (m), 1608 (w), 1558 (w), 1541 (w), 1507 (w), 1458 (m), 1417 (w), 1362 (m), 1338 (w), 1300 (w), 1267 (m), 1252 (m), 1201 (w), 1097 (w), 1071 (m), 1016 (w), 986 (w), 917 (m), 880 (m), 817 (s), 784 (s), 756 (w), 728 (w), 718 (w), 683 (w), 668 (w) cm^{-1}; UV/Vis (CH_2Cl_2): λ_{max} (log ε) = 308 (4.70), 315 sh (4.68), 338 (3.64), 367 (3.66), 386 (3.69), 408 (3.50), 537 sh (2.65), 590 (2.70), 645 (2.71), 722 sh (2.64), 823 sh (2.47) nm; UV/Vis (10% TFA/CH_2Cl_2): λ_{max} (log ε) = 278 (4.26), 372 sh (4.08), 412 (4.31) nm; ^{1}H NMR (500 MHz, $CDCl_3$): δ_H = 8.31 (d, *J* = 1.7 Hz, 1H, 4-H), 8.02 (d, *J* = 8.2 Hz, 1H, 5-H), 7.79 (dd, *J* = 8.3, 1.7 Hz, 1H, 2-H), 7.73 (d, *J* = 8.3 Hz, 1H, 1-H), 7.66 (d, *J* = 0.9 Hz, 1H, 9-H), 6.96 (d, *J* = 11.7 Hz, 1H, 7-H), 6.85 (dd, *J* = 11.7, 8.2 Hz, 1H, 6-H), 2.91 (t, *J* = 6.9 Hz, 1H, *i*-Pr), 2.59 (s, 3H, Me), 1.49 (s, 9H, *t*-Bu), 1.33 (d, *J* = 6.9 Hz, 6H, *i*-Pr) ppm; ^{13}C NMR (125 MHz, $CDCl_3$): δ_C = 144.8, 141.5, 141.1, 140.9, 134.7, 133.0, 130.4, 129.2, 126.5, 124.9, 124.7, 121.9, 117.5, 116.4, 38.7, 35.1, 32.0, 23.9, 10.2 ppm; HRMS (MALDI–TOF, positive) calcd for $C_{22}H_{26}^+$ $[M]^+$ 290.2029, found 290.2034.

Compound 8: Trifluoroacetic anhydride (1.67 g, 7.95 mmol) was added at room temperature to a solution of **2b** (1.04 g, 3.71 mmol) in $CHCl_3$ (37 mL) and pyridine (4 mL), and the resulting mixture was stirred at room temperature for 40 min. After the solvent was removed under reduced pressure, the crude product was purified by column chromatography on silica gel with $CHCl_3$ as an eluent to give **8** (1.33 g, 95%) as a brown

solid. M.p. 54–60 °C; IR (AT-IR): ν_{max} = 2961 (w), 1635 (m), 1530 (w), 1460 (w), 1429 (s), 1395 (w), 1365 (w), 1333 (w), 1307 (w), 1265 (m), 1248 (m), 1193 (s), 1136 (s), 1073 (w), 1041 (m), 1007 (w), 986 (w), 961 (w), 928 (w), 866 (w), 810 (w), 795 (w), 760 (m), 726 (m), 709 (w), 695 (w), 683 (w), 673 (w), 655 (w) cm^{-1}; ^1H NMR (500 MHz, $CDCl_3$): δ_H = 9.49 (d, *J* = 1.4 Hz, 1H, 9-H), 8.18 (d, *J* = 9.9 Hz, 1H, 5-H), 7.72 (dd, *J* = 9.9, 1.4 Hz, 1H, 7-H), 7.50 (t, *J* = 9.9 Hz, 1H, 6-H), 3.46 (m, 1H, *c*-Hex), 3.20 (sept, *J* = 7.0 Hz, 1H, *i*-Pr), 3.12–3.06 (m, 2H, *c*-Hex), 2.63–2.57 (m, 1H, *c*-Hex), 2.19–2.16 (m, 1H, *c*-Hex), 1.63–1.57 (m, 1H, *c*-Hex), 1.41–1.39 (m, 7H, *i*-Pr, *c*-Hex), 1.03 (s, 9H, *t*-Bu) ppm; ^{13}C NMR (125 MHz, $CDCl_3$): δ_C = 176.4 (q, *J* = 34.8 Hz, $COCF_3$), 153.4, 152.5, 145.2, 142.8, 137.4, 136.9, 131.6, 128.8, 128.4, 117.5 (q, *J* = 290.3 Hz, CF_3), 115.6, 44.5, 39.6, 32.7, 28.0, 27.9, 27.4, 25.2, 24.6, 24.5, 24.3 ppm; HRMS (MALDI–TOF, positive) calcd for $C_{23}H_{27}F_3O$ + H^+ $[M + H]^+$ 377.2087, found 377.2060.

Compound 9: DDQ (1.37 g, 6.04 mmol) was added at 0 °C to a solution of **8** (748 mg, 1.99 mmol) in toluene (30 mL). The resulting mixture was stirred at room temperature for 1.5 h. The reaction mixture was poured into K_2CO_3 aq., extracted with toluene, washed with brine, and dried with Na_2SO_4. The crude product was purified by column chromatography on silica gel with toluene as an eluent to give **9** (639 mg, 86%) as a brown solid. M.p. 128–130 °C; IR (AT-IR): ν_{max} = 2963 (w), 1632 (m), 1611 (w), 1509 (w), 1482 (w), 1463 (m), 1419 (w), 1367 (w), 1333 (w), 1281 (w), 1265 (m), 1254 (m), 1244 (m), 1225 (w), 1191 (m), 1182 (m), 1127 (s), 1070 (m), 1049 (s), 1000 (w), 958 (m), 898 (w), 877 (w), 820 (m), 798 (m), 772 (w), 738 (w), 704 (w), 673 (w), 656 (w) cm^{-1}; UV/Vis (CH_2Cl_2): λ_{max} (log ε) = 249 (4.38), 293 (4.58), 349 sh (4.30), 362 (4.35), 454 (4.04) nm; UV/Vis (10% TFA/CH_2Cl_2): λ_{max} (log ε) = 286 (4.26), 310 sh (4.15), 366 (4.25), 406 sh (4.07), 474 sh (3.61) nm; ^1H NMR (500 MHz, $CDCl_3$): δ_H = 9.88 (d, *J* = 1.7 Hz, 1H, 9-H), 8.89 (d, *J* = 8.3 Hz, 1H, 5-H), 8.38 (d, *J* = 2.0 Hz, 1H, 4-H), 8.27 (d, *J* = 8.6 Hz, 1H, 1-H), 7.86–7.82 (m, 2H, 2-H, 7-H), 7.73 (dd, *J* = 10.9, 8.3 Hz, 1H, 6-H),

3.26 (sept, *J* = 6.9 Hz, 1H, *i*-Pr), 1.48 (s, 9H, *t*-Bu), 1.45 (d, *J* = 6.9 Hz, 6H, *i*-Pr) ppm; ^{13}C NMR (125 MHz, $CDCl_3$): δ_C = 176.3 (q, *J* = 35.2 Hz, $COCF_3$), 155.7, 149.0, 146.3, 143.9, 139.9, 138.0, 136.7, 131.8, 131.1, 130.8, 129.5, 121.0, 117.8 (q, *J* = 289.9 Hz, CF_3), 116.8, 113.1, 39.9, 35.0, 31.7, 24.5 ppm; HRMS (MALDI–TOF, positive) calcd for $C_{23}H_{23}F_3O^+$ $[M]^+$ 372.1696, found 372.1690.

Compound 10: $NaBH_4$ (92 mg, 2.43 mmol) was added to a solution of **9** (545 mg, 1.46 mmol) in THF (6 mL) and diglyme (1.5 mL), and the resulting mixture was stirred for 1 h. Then, $NaBH_4$ (84 mg, 2.22 mmol) and $BF_3{\cdot}Et_2O$ (0.7 mL) was added to the reaction mixture, and the resulting mixture was stirred for 2 h. The reaction mixture was poured into water, extracted with toluene, washed with brine, and dried with Na_2SO_4. The crude product was purified by silica gel column chromatography with hexane/toluene (2:1) as an eluent to give **10** (376 mg, 38%) as a green solid. M.p. 128–130 °C; IR (AT-IR): ν_{max} = 2965 (w), 1698 (w), 1609 (w), 1521 (w), 1463 (w), 1395 (w), 1364 (w), 1254 (w), 1216 (w), 1164 (s), 1123 (s), 1081 (m), 1002 (w), 926 (w), 883 (w), 862 (w), 836 (w), 790 (m), 758 (s), 679 (w), 665 (w) cm^{-1}; UV/Vis (CH_2Cl_2): λ_{max} (log ε) = 238 (4.15), 306 (4.55), 370 (3.59), 388 (3.61), 409 (3.51), 573 (2.66), 623 (2.66), 702 sh (2.60) nm; UV/Vis (10% TFA/CH_2Cl_2): λ_{max} (log ε) = 270 (4.24), 291 sh (4.10), 306 (4.18), 372 sh (4.03), 406 (4.14) nm; ^{1}H NMR (500 MHz, $CDCl_3$): δ_H = 8.33 (s, 2H, 4-H), 8.21 (d, *J* = 8.0 Hz, 2H, 5-H), 8.03 (d, *J* = 8.6 Hz, 2H, 1-H), 7.75 (m, 4H, 2-H, 9-H), 7.02 (d, *J* = 11.5 Hz, 2H, 7-H), 6.93–6.97 (m, 2H, 6-H), 6.15 (q, *J* = 11.8 Hz, 1H, CH), 2.62 (sept, *J* = 6.9 Hz, 2H, *i*-Pr), 1.47 (s, 18H, *t*-Bu), 0.97 (d, *J* = 6.9 Hz, 6H, *i*-Pr), 0.92 (d, *J* = 6.9 Hz, 6H, *i*-Pr) ppm; ^{13}C NMR (125 MHz, $CDCl_3$): δ_C = 144.5, 143.8, 141.4, 139.6, 136.0, 135.5, 130.6, 129.5, 128.1 (q, *J* = 280.7 Hz, CF_3), 127.4, 126.2, 125.6, 119.1, 118.0, 116.5, 42.1 (d, *J* = 30.0 Hz, CH), 38.7, 35.0, 31.9, 23.8, 23.7 ppm; HRMS (MALDI–TOF, Positive) calcd for $C_{44}H_{47}F_3^+$ $[M]^+$ 632.3624, found 632.3601; HRMS (MALDI–TOF, positive) calcd for $C_{44}H_{47}F_3 + Ag^+$ $[M + Ag]^+$ 739.2675, found 739.2698.

Compound 11: 1M MeONa in MeOH (40 mL) was added to a solution of **8** (685 mg, 1.82 mmol) in MeOH (10 mL). The resulting mixture was refluxed for 23 h. After cooling to room temperature, the reaction mixture was poured into NH_4Cl aq., extracted with toluene, washed with brine, and dried with Na_2SO_4. The crude product was purified by column chromatography on silica gel with toluene/AcOEt (4:1) as an eluent to give **11** (283 mg, 46%) as purple oil. IR (AT-IR): ν_{max} = 2958 (m), 1682 (m), 1525 (w), 1464 (m), 1442 (s), 1420 (m), 1389 (m), 1379 (m), 1364 (m), 1331 (w), 1299 (w), 1217 (s), 1189 (m), 1171 (m), 1117 (m), 1068 (w), 1025 (m), 957 (w), 923 (w), 885 (w), 829 (w), 781 (m), 757 (m), 735 (w), 693 (w), 675 (w), 666 (m) cm^{-1}; ^1H NMR (500 MHz, $CDCl_3$): δ_H = 9.61 (s, 1H, 9-H), 8.13 (d, *J* = 10.0 Hz, 1H, 5-H), 7.61 (d, *J* = 10.0 Hz, 1H, 7-H), 7.32 (t, *J* = 10.0 Hz, 1H, 6-H), 3.95 (s, 3H, CO_2Me), 3.61–3.57 (m, 1H, *c*-Hex), 3.20–3.06 (m, 3H, *i*-Pr, *c*-Hex), 2.63–2.58 (m, 1H, *c*-Hex), 2.18–2.14 (m, 1H, *c*-Hex), 1.56–1.54 (m, 1H, *c*-Hex), 1.45–1.34 (m, 7H, *i*-Pr, *c*-Hex), 1.03 (s, 9H, *t*-Bu) ppm; ^{13}C NMR (125 MHz, $CDCl_3$): δ_C = 166.9, 153.8, 148.3, 142.2, 139.8, 136.0, 135.4, 130.8, 126.2, 125.5, 111.4, 50.7, 45.0, 39.4, 32.7, 29.0, 27.6, 25.3, 24.83, 24.81, 24.3 ppm; HRMS (MALDI–TOF, positive) calcd for $C_{23}H_{30}O_2^+$ $[M]^+$ 338.2240, found 338.2222.

Compound 12: DDQ (254 mg, 1.12 mmol) was added at 0 °C to a solution of **11** (122 mg, 0.360 mmol) in toluene (20 mL). The resulting mixture was stirred at room temperature for 2 h. The reaction mixture was poured into K_2CO_3 aq. and extracted with toluene. The organic layer was washed with brine, dried with Na_2SO_4, and concentrated under reduced pressure. The crude product was purified by column chromatography on silica gel with toluene to give **12** (104 mg, 86%) as a green solid. M.p. 131 °C; IR (AT-IR): ν_{max} = 2959 (w), 2869 (w), 1678 (s), 1608 (w), 1545 (w), 1507 (m), 1468 (s), 1409 (m), 1370 (m), 1333 (w), 1301 (w), 1272 (w), 1254 (m), 1196 (s), 1173 (s), 1140 (m), 1127 (m), 1095 (m), 1065 (w), 1050 (w), 1019

(m), 998 (w), 968 (w), 945 (w), 927 (w), 879 (w), 842 (m), 828 (m), 795 (m), 756 (m), 720 (w), 670 (w) cm^{-1}; UV/Vis (CH_2Cl_2): λ_{max} (log ε) = 266 (4.45), 331 (4.54), 344 (4.54), 384 sh (3.75), 406 (3.82), 427 (3.85), 536 (2.86), 591 (2.85), 641 sh (2.78), 716 sh (2.62) nm; UV/Vis (10% TFA/CH_2Cl_2): λ_{max} (log ε) = 277 (4.15), 307 sh (3.55), 368 sh (4.12), 410 (4.23) nm; ^{1}H NMR (500 MHz, $CDCl_3$): δ_H = 9.66 (d, *J* = 1.7 Hz, 1H, 9-H), 8.67 (dd, *J* = 8.6, 0.9 Hz, 1H, 5-H), 8.44 (d, *J* = 8.6 Hz, 1H, 1-H), 8.36 (d, *J* = 1.5 Hz, 1H, 4-H), 7.83 (dd, *J* = 8.6, 1.5 Hz, 1H, 2-H), 7.58–7.55 (m, 1H, 7-H), 7.43 (dd, *J* = 11.0, 8.6 Hz, 1H, 6-H), 4.07 (s, 3H, CO_2Me), 3.18 (sept, *J* = 6.9 Hz, 1H, *i*-Pr), 1.48 (s, 9H, *t*-Bu), 1.42 (d, *J* = 6.9 Hz, 6H, *i*-Pr) ppm; ^{13}C NMR (125 MHz, $CDCl_3$): δ_C = 167.3, 150.2, 145.4, 144.6, 142.3, 139.3, 137.9, 134.4, 130.2, 130.1, 128.3, 128.1, 121.9, 116.3, 110.7, 51.0, 39.5, 35.0, 31.9, 24.4 ppm; HRMS (MALDI–TOF, positive) calcd for $C_{23}H_{26}O_2^+$ $[M]^+$ 334.1927, found 334.1945.

Compound 13: A solution of **12** (229 mg, 0.685 mmol) in 100% H_3PO_4 (20 mL) was stirred at 100 °C for 1.5 h. After cooling to room temperature, the reaction mixture was poured into water, extracted with toluene, washed with brine, and dried with Na_2SO_4. The crude product was purified by alumina column chromatography with hexane as an eluent to give **13** (149 mg, 79%) as a blue solid. M.p. 72–75 °C; IR (AT-IR): ν_{max} = 2958 (s), 2925 (s), 2852 (m), 1698 (w), 1607 (w), 1508 (w), 1462 (s), 1415 (w), 1362 (m), 1253 (m), 1073 (w), 1000 (w), 923 (w), 880 (w), 823 (m), 786 (m), 754 (w), 719 (w), 702 (w), 688 (w), 665 (w), 656 (w) cm^{-1}; UV/Vis (CH_2Cl_2): λ_{max} (log ε) = 253 (4.08), 306 (4.74), 363 (3.71), 382 (3.73), 402 (3.47), 525 sh (2.65), 570 (2.74), 628 (2.78), 699 (2.70), 781 sh (2.57) nm; UV/Vis (10% TFA/CH_2Cl_2): λ_{max} (log ε) = 276 (4.29), 370 sh (4.12), 406 (4.38) nm; ^{1}H NMR (500 MHz, $CDCl_3$): δ_H = 8.33 (d, *J* = 0.9 Hz, 1H, 4-H), 8.22 (d, *J* = 8.3 Hz, 1H, 5-H), 7.81 (d, *J* = 1.7 Hz, 1H, 9-H), 7.72–7.77 (m, 2H, 1-H, 2-H), 7.18 (br s, 1H, 10-H), 7.11 (dd, *J* = 11.5, 1.7 Hz, 1H, 7-H), 6.99 (dd, *J* = 11.5, 8.3 Hz, 1H, 6-H), 2.92 (sept, *J* = 6.9 Hz, 1H, *i*-Pr), 1.47 (s, 9H, *t*-Bu), 1.32 (d, *J* = 6.9 Hz, 6H, *i*-Pr) ppm; ^{13}C NMR (125 MHz, $CDCl_3$): δ_C = 144.5, 142.4, 140.8,

140.6, 139.0, 135.6, 132.6, 131.2, 126.8, 126.7, 124.8, 119.6, 116.7, 115.0, 38.4, 35.1, 32.0, 23.9 ppm; HRMS (MALDI–TOF, positive) calcd for $C_{21}H_{24}$ + H^+ $[M + H]^+$ 277.1946, found 277.1959.

Compound 14: TFAA (256 mg, 1.22 mmol) was added to a solution of **2b** (145 mg, 0.517 mmol) and in DMSO (0.5 mL) and CH_2Cl_2 (5 mL). The resulting mixture was stirred at room temperature for 15 min. After the solvent was removed under reduced pressure, Et_3N (10 mL) was added, and the resulting mixture was refluxed for 2 h. After cooling to room temperature, the solvent was removed under reduced pressure. The crude product was purified by column chromatography on silica gel with hexane/toluene (1:1) as an eluent to give **14** (160 mg, 95%) as blue oil. IR (AT-IR): ν_{max} = 2957 (s), 2917 (m), 2867 (m), 1576 (m), 1518 (w), 1465 (s), 1436 (m), 1419 (m), 1394 (s), 1363 (m), 1328 (w), 1303 (w), 1276 (w), 1240 (m), 1224 (w), 1161 (w), 1096 (w), 1032 (w), 963 (m), 912 (m), 863 (w), 817 (w), 785 (s), 758 (s), 736 (m), 688 (w), 679 (w), 659 (w) cm^{-1}; ^1H NMR (500 MHz, $CDCl_3$): δ_H = 8.64 (d, *J* = 1.4 Hz, 1H, 9-H), 8.02 (d, *J* = 9.5 Hz, 1H, 5-H), 7.48 (d, *J* = 10.3 Hz, 1H, 7-H), 7.11 (t, *J* = 9.9 Hz, 1H, 6-H), 3.43–3.38 (m, 1H, *c*-Hex), 3.24–3.20 (m, 1H, *c*-Hex), 3.16 (sept, *J* = 6.9 Hz, 1H, *i*-Pr), 2.99–2.92 (m, 1H, *c*-Hex), 2.71–2.65 (m, 1H, *c*-Hex), 2.28 (s, 3H, SMe), 2.25–2.21 (m, 1H, *c*-Hex), 1.66–1.59 (m, 1H, *c*-Hex), 1.53–1.45 (m, 1H, *c*-Hex), 1.40 (d, *J* = 6.9 Hz, 6H, *i*-Pr), 1.05 (s, 9H, *t*-Bu) ppm; ^{13}C NMR (125 MHz, $CDCl_3$): δ_C = 153.3, 143.3, 140.7, 136.6, 135.2, 132.8, 129.8, 125.0, 122.4, 115.3, 45.7, 38.8, 32.8, 27.6, 26.9, 25.2, 24.7, 24.2, 20.6 ppm; HRMS (MALDI–TOF, positive) calcd for $C_{22}H_{30}S^+$ $[M]^+$ 326.2063, found 326.2040.

Compound 15: DDQ (193 mg, 0.850 mmol) was added at 0 °C to a solution of **14** (137 mg, 0.420 mmol) in toluene (10 mL). The resulting mixture was stirred at room temperature for 1 h. The reaction mixture was poured into K_2CO_3 aq. and extracted with toluene. The organic

layer was washed with brine, dried with Na_2SO_4, and concentrated under reduced pressure. The crude product was purified by column chromatography on silica gel with toluene/EtOAc (5:1) as an eluent to give **15** (126 mg, 93%) as green oil. IR (AT-IR): ν_{max} = 2957 (s), 2921 (m), 2866 (m), 1608 (m), 1557 (w), 1506 (m), 1461 (s), 1415 (m), 1389 (m), 1362 (m), 1331 (w), 1297 (m), 1268 (m), 1252 (m), 1237 (m), 1205 (m), 1065 (m), 1003 (m), 973 (m), 955 (m), 930 (m), 878 (m), 828 (m), 787 (s), 756 (m), 741 (w), 713 (m), 685 (m), 670 (m), 661 (m), 653 (m) cm^{-1}; UV/Vis (CH_2Cl_2): λ_{max} (log ε) = 264 (4.03), 319 (4.43), 373 (3.51), 392 (3.58), 414 (3.49), 525 sh (2.44), 580 (2.48), 627 (2.49), 694 sh (2.39) nm; UV/Vis (10% TFA/CH_2Cl_2): λ_{max} (log ε) = 306 (3.69), 367 (4.00), 401 (4.00) nm; ^{1}H NMR (500 MHz, $CDCl_3$): δ_H = 8.35 (dd, *J* = 14.6, 1.4 Hz, 2H, 9-H, 4-H), 8.25 (dd, *J* = 8.4, 0.7 Hz, 1H, 5-H), 7.99 (dd, *J* = 8.3, 0.6 Hz, 1H, 1-H), 7.83 (dd, *J* = 8.3, 1.7 Hz, 1H, 2-H), 7.20 (dd, *J* = 11.5, 0.9 Hz, 1H, 7-H), 7.08 (dd, *J* = 11.5, 8.3 Hz, 1H, 6-H), 3.04 (sept, *J* = 6.9 Hz, 1H, *i*-Pr), 2.39 (s, 3H, SMe), 1.49 (s, 9H, *t*-Bu), 1.37 (d, *J* = 6.9 Hz, 6H, *i*-Pr) ppm; ^{13}C NMR (125 MHz, $CDCl_3$): δ_C = 145.4, 144.3, 141.2, 140.9, 140.5, 136.0, 131.4, 130.2, 127.2, 126.9, 125.8, 118.6, 117.1, 116.6, 38.7, 35.1, 32.0, 24.0, 19.0 ppm; HRMS (MALDI–TOF, positive) calcd for $C_{22}H_{26}S^+$ $[M]^+$ 322.1750, found 322.1739.

Compound 17a: NIS (340 mg, 1.51 mmol) was added to a solution of **2b** (280 mg, 1.00 mmol) in CH_2Cl_2 (10 mL) and Et_3N (1 mL) at 0 °C. The mixture was stirred at room temperature for 30 min. The reaction mixture was poured into saturated Na_2SO_3 aq., extracted with CH_2Cl_2, washed with brine, and dried with Na_2SO_4. The crude product was passed though the short alumina column with hexane as an eluent to give **16**. To a degassed solution of **16** (406 mg, 1.00 mmol), phenylboronic acid (193 mg, 1.58 mmol), K_3PO_4 (669 mg, 3.15 mmol) in 1,4-dioxane (5 mL) and H_2O (0.5 mL) were added $PdCl_2$(dppf) (56 mg, 0.07 mmol). The resulting mixture was refluxed for 18 h. The reaction mixture was poured into water, extracted with toluene, washed with brine, and dried with Na_2SO_4. The crude

product was purified by column chromatography on silica gel with hexane as an eluent to give **17a** (299 mg, 84%) as blue oil. IR (AT-IR): ν_{max} = 2956 (m), 2868 (w), 1599 (w), 1573 (w), 1498 (w), 1465 (m), 1444 (m), 1392 (m), 1363 (m), 1326 (w), 1241 (w), 1174 (w), 1072 (w), 1030 (w), 957 (w), 920 (w), 829 (w), 782 (m), 761 (s), 723 (w), 702 (s), 680 (w), 666 (w) cm^{-1}; ^1H NMR (500 MHz, $CDCl_3$): δ_H = 8.26 (s, *J* = 1.1 Hz, 1H, 9-H), 8.10 (d, *J* = 9.5 Hz, 1H, 5-H), 7.51–7.55 (m, 4H, Ph), 7.44 (d, *J* = 10.3 Hz, 1H, 7-H), 7.39 (td, *J* = 5.7, 3.0 Hz, 1H, Ph), 7.06 (t, *J* = 9.9 Hz, 1H, 6-H), 3.36–3.32 (m, 1H, *c*-Hex), 3.17–3.13 (m, 1H, *c*-Hex), 3.10–3.00 (m, 2H, *i*-Pr, *c*-Hex), 2.83–2.77 (m, 1H, *c*-Hex), 2.21–2.17 (m, 1H, *c*-Hex), 1.75–1.70 (m, 1H, *c*-Hex), 1.53–1.44 (m, 1H, *c*-Hex), 1.32 (d, *J* = 6.9 Hz, 3H, *i*-Pr), 1.31 (d, *J* = 6.9 Hz, 3H, *i*-Pr), 1.09 (s, 9H, *t*-Bu) ppm; ^{13}C NMR (125 MHz, $CDCl_3$): δ_C = 148.5, 142.4, 136.9, 136.2, 135.7, 135.1, 133.1, 130.6, 129.9, 128.3, 126.1, 126.0, 124.8, 121.3, 45.7, 38.8, 32.9, 27.6, 27.4, 25.6, 24.7, 24.45, 24.37 ppm, one signal is overlapped with other signal; HRMS (MALDI–TOF, positive) calcd for $C_{27}H_{32}^+$ $[M]^+$ 356.2499, found 356.2519.

Compound 18a: DDQ (271 mg, 1.19 mmol) was added at 0 °C to a solution of **17a** (110 mg, 0.312 mmol) in toluene (15 mL). The resulting mixture was stirred at room temperature for 1.5 h. The reaction mixture was poured into K_2CO_3 aq., extracted with toluene, washed with brine, and dried with Na_2SO_4. The crude product was purified by column chromatography on silica gel with toluene as an eluent to give **18a** (74 mg, 67%) as green oil. IR (AT-IR): ν_{max} = 3567 (w), 2960 (m), 1541 (w), 1522 (w), 1507 (w), 1489 (w), 1472 (w), 1457 (m), 1362 (w), 1253 (w), 1001 (w), 824 (m), 787 (m), 756 (m), 731 (m), 702 (s) cm^{-1}; UV/Vis (CH_2Cl_2): λ_{max} (log ε) = 252 (4.27), 319 (4.59), 375 (3.72), 393 (3.80), 416 (3.70), 536 sh (2.66), 587 (2.73), 642 (2.75), 721 sh (2.69) nm; UV/Vis (10% TFA/CH_2Cl_2): λ_{max} (log ε) = 274 (4.24), 347 sh (3.96), 386 (4.17), 420 (4.18) nm; ^1H NMR (500 MHz, $CDCl_3$): δ_H = 8.40 (d, *J* = 1.4 Hz, 1H, 4-H), 8.26 (d, *J* = 8.3 Hz, 1H, 5-H), 7.98 (s, 1H, 9-H), 7.82 (d, *J* = 8.3 Hz, 1H, 2-H), 7.76 (dd, *J* = 8.3, 1.7 Hz, 1H, 1-H), 7.67 (dd, *J* = 8.0, 1.1 Hz, 2H, Ph), 7.56 (t, *J* = 7.7 Hz, 2H, Ph),

7.40–7.43 (m, 1H, Ph), 7.10 (d, *J* = 11.7 Hz, 1H, 7-H), 6.99 (dd, *J* = 11.5, 8.0 Hz, 1H, 6-H), 2.85 (sept, *J* = 6.7 Hz, 1H, *i*-Pr), 1.50 (s, 9H, *t*-Bu), 1.26 (d, *J* = 6.9 Hz, 6H, *i*-Pr) ppm; ^{13}C NMR (125 MHz, $CDCl_3$): δ_C = 145.2, 143.1, 141.4, 140.1, 136.3, 136.0, 133.9, 130.5, 130.4, 130.1, 128.7, 126.94, 126.86, 126.8, 126.7, 125.2, 118.7, 116.6, 38.7, 35.1, 32.0, 23.8 ppm; HRMS (MALDI–TOF, positive) calcd for $C_{27}H_{28}^+$ $[M]^+$ 352.2186, found 352.2206.

Compound 17b: NIS (337 mg, 1.50 mmol) was added to a solution of **2b** (282 mg, 1.01 mmol) in CH_2Cl_2 (10 mL) and Et_3N (1 mL) at 0 °C. The mixture was stirred at room temperature for 30 min. The reaction mixture was poured into saturated Na_2SO_3 aq., extracted with CH_2Cl_2, washed with brine, and dried with Na_2SO_4. The crude product was passed though the short alumina column with hexane as an eluent to give **16**. To a degassed solution of **16** (410 mg, 1.01 mmol), 4-*tert*-butylphenylboronic acid (269 mg, 1.51 mmol), K_3PO_4 (638 mg, 3.01 mmol) in 1,4-dioxane (5 mL) and H_2O (0.5 mL) were added $PdCl_2$(dppf) (41 mg, 0.05 mmol). The resulting mixture was refluxed for 14 h. The reaction mixture was poured into water, extracted with toluene, washed with brine, and dried with Na_2SO_4, and concentrated under reduced pressure. The crude product was purified by column chromatography on silica gel with hexane as an eluent to give **17b** (329 mg, 79%) as blue oil. IR (AT-IR): ν_{max} = 2957 (m), 1574 (w), 1509 (w), 1464 (m), 1392 (m), 1363 (m), 1326 (w), 1268 (w), 1242 (w), 1114 (w), 1021 (w), 923 (w), 849 (m), 817 (m), 783 (m), 757 (s), 713 (w), 686 (w), 673 (w), 664 (w) cm^{-1}; ^{1}H NMR (500 MHz, $CDCl_3$): δ_H = 8.26 (s, 1H, 9-H), 8.04 (d, *J* = 9.7 Hz, 1H, 5-H), 7.51 (d, *J* = 8.3 Hz, 2H, Ph), 7.39–7.42 (m, 3H, 7-H, Ph), 7.01 (t, *J* = 9.7 Hz, 1H, 6-H), 3.31–3.27 (m, 1H, *c*-Hex), 3.15–3.10 (m, 1H, *c*-Hex), 2.97–3.06 (m, 2H, *i*-Pr, *c*-Hex), 2.78–2.72 (m, 1H, *c*-Hex), 2.16–2.13 (m, 1H, *c*-Hex), 1.70–1.65 (m, 1H, *c*-Hex), 1.44–1.41 (m, 10H, *t*-Bu, *c*-Hex), 1.29 (d, *J* = 6.9 Hz, 3H, *i*-Pr), 1.28 (d, *J* = 6.9 Hz, 3H, *i*-Pr), 1.04 (s, 9H, *t*-Bu) ppm; ^{13}C NMR (125 MHz, $CDCl_3$): δ_C = 148.6, 148.5, 142.2, 136.0, 135.7, 134.9, 133.8, 133.4, 130.2, 129.8, 126.1, 125.2, 124.7, 121.2, 45.7, 38.8, 34.7, 32.9, 31.6,

27.6, 27.5, 25.6, 24.8, 24.5, 24.4 ppm; HRMS (MALDI–TOF, positive) calcd for $C_{31}H_{40}^{+}$ $[M]^{+}$ 412.3125, found 412.3108.

Compound 18b: DDQ (227 mg, 0.998 mmol) was added to a solution of **17b** (205 mg, 0.498 mmol) in toluene (15 mL) at 0 °C. The resulting mixture was stirred at room temperature for 1.5 h. The reaction mixture was poured into K_2CO_3 aq., extracted with toluene, washed with brine, and dried with Na_2SO_4. The crude product was purified by column chromatography on silica gel with toluene as an eluent to give **18b** (107 mg, 53%) as green oil. IR (AT-IR): ν_{max} = 2961 (m), 1609 (w), 1531 (w), 1462 (m), 1416 (w), 1362 (m), 1268 (w), 1200 (w), 1106 (w), 1061 (w), 1022 (w), 1001 (w), 948 (w), 927 (w), 880 (w), 863 (w), 829 (s), 787 (m), 760 (m), 703 (w), 692 (w), 682 (w), 667 (w) cm^{-1}; UV/Vis (CH_2Cl_2): λ_{max} (log ε) = 265 sh (4.30), 279 sh (4.34), 320 (4.54), 375 (3.68), 395 (3.77), 418 (3.67), 543 (2.55), 591 (2.59), 657 (2.63), 734 (2.51) nm; UV/Vis (10% TFA/CH_2Cl_2): λ_{max} (log ε) = 275 (4.18), 359 sh (4.01), 388 (4.17), 434 sh (3.97) nm; ^{1}H NMR (500 MHz, $CDCl_3$): δ_H = 8.37 (d, *J* = 1.5 Hz, 1H, 4-H), 8.20–8.22 (m, 1H, 5-H), 7.99 (s, 1H, 9-H), 7.84 (d, *J* = 8.3 Hz, 1H, 1-H), 7.73 (dd, *J* = 8.3, 1.5 Hz, 1H, 2-H), 7.58 (m, 4H, Ph), 7.07 (d, *J* = 11.7 Hz, 1H, 7-H), 6.96 (dd, *J* = 11.7, 8.3 Hz, 1H, 6-H), 2.85 (sept, *J* = 6.9 Hz, 1H), 1.48 (s, 9H, *t*-Bu), 1.43 (s, 9H, *t*-Bu), 1.25 (d, *J* = 6.9 Hz, 6H, *i*-Pr) ppm; ^{13}C NMR (125 MHz, $CDCl_3$): δ_C = 149.5, 145.1, 142.8, 141.5, 140.2, 135.7, 133.7, 133.2, 130.9, 130.5, 129.6, 126.9, 126.7, 126.6, 125.6, 125.1, 118.9, 116.6, 38.7, 35.1, 34.8, 32.0, 31.6, 23.9 ppm; HRMS (MALDI–TOF, positive) calcd for $C_{31}H_{36}^{+}$ $[M]^{+}$ 408.2812, found: 408.2797.

Compound 20: NBS (5.34 mg, 30.0 mmol) was added to a solution of **19** (2.40 g, 10.0 mmol) in $CHCl_3$ (100 mL) and the resulting mixture was refluxed for 6 h. The solvent was removed under reduced pressure and the crude product was purified by column chromatography on silica gel with toluene/EtOAc (5:1) as an eluent to give **20** (1.51 g, 48%)

as a green solid. M.p. 149 °C; IR (AT-IR): ν_{max} = 1687 (m), 1593 (w), 1524 (w), 1487 (w), 1468 (m), 1444 (m), 1405 (m), 1378 (w), 1343 (w), 1317 (w), 1275 (w), 1256 (w), 1216 (w), 1184 (s), 1172 (s), 1132 (m), 1061 (w), 1018 (m), 962 (w), 948 (w), 915 (w), 888 (w), 864 (w), 839 (w), 816 (s), 783 (w), 740 (w), 696 (m) cm^{-1}; UV/Vis (CH_2Cl_2): λ_{max} (log ε) = 267 (4.49), 325 (4.57), 338 (4.60), 378 sh (3.74), 399 (3.86), 424 (3.91), 534 (2.71), 579 (2.73), 640 sh (2.59), 705 sh (2.30) nm; UV/Vis (10% TFA/CH_2Cl_2): λ_{max} (log ε) = 289 (4.22), 363 (4.27), 421 sh (3.78) nm; ^{1}H NMR (500 MHz, $CDCl_3$): δ_H = 9.54 (d, *J* = 11.2 Hz, 1H, 9-H), 8.61 (d, *J* = 8.6 Hz, 1H, 5-H), 8.46 (d, *J* = 2.0 Hz, 1H, 4-H), 8.40 (d, *J* = 8.6 Hz, 1H, 1-H), 7.80 (dd, *J* = 8.6, 1.7 Hz, 1H, 2-H), 7.64 (dd, *J* = 10.3, 9.2 Hz, 1H, 7-H), 7.44–7.48 (m, 2H, 6-H, 8-H), 4.05 (s, 3H, CO_2Me) ppm; ^{13}C NMR (125 MHz, $CDCl_3$): δ_C = 166.6, 144.2, 140.8, 139.4, 138.3, 137.5, 132.7, 132.3, 131.9, 130.0, 128.9, 123.9, 123.4, 116.5, 111.9, 51.3 ppm; HRMS (MALDI–TOF, positive) calcd for $C_{16}H_{11}BrO_2^+$ $[M]^+$ 313.9942, found 313.9949.

Compound 21: A solution of **20** (731 mg, 2.00 mmol) in 100% H_3PO_4 (40 mL) was stirred at 100 °C for 30 min. After cooling to room temperature, the reaction mixture was poured into water, neutralized with KOH aq. The precipitate was collected by filtration and dissolved in $CHCl_3$. The crude product was purified by silica gel column chromatography with hexane/toluene (1:1) as an eluent to give **21** (108 mg, 21%) as green crystals. M.p. 134–135 °C; IR (AT-IR): ν_{max} = 1596 (w), 1463 (w), 1434 (m), 1387 (w), 1374 (w), 1325 (w), 1294 (w), 1272 (w), 1263 (w), 1234 (w), 1205 (w), 1118 (w), 1056 (w), 1044 (w), 973 (w), 938 (w), 918 (w), 878 (w), 859 (w), 841 (w), 826 (s), 802 (w), 785 (w), 771 (w), 743 (m), 713 (w), 690 (s), 655 (w) cm^{-1}; UV/Vis (CH_2Cl_2): λ_{max} (log ε) = 260 (4.12), 307 (4.74), 319 sh (4.66), 361 (3.72), 381 (3.81), 401 (3.71), 525 (2.56), 567 (2.65), 619 (2.67), 683 sh (2.56), 771 sh (2.32) nm; UV/Vis (10% TFA/CH_2Cl_2): λ_{max} (log ε) = 274 (4.29), 367 (4.16), 401 (4.11) nm; ^{1}H NMR (500 MHz, $CDCl_3$): δ_H = 8.47 (s, 1H, 4-H), 8.24 (d, *J* = 8.3 Hz, 1H, 9-H), 7.94 (d, *J* = 10.9 Hz, 1H, 5-H), 7.72–7.74 (m, 2H, 1-H, 2-H), 7.21–7.27 (m, 2H, 7-H, 10-H), 7.04 (dd, *J* =

11.2, 8.3 Hz, 1H, 8-H), 6.87 (dd, *J* = 10.9, 8.6 Hz, 1H, 6-H) ppm; ^{13}C NMR (125 MHz, $CDCl_3$): δ_C = 140.8, 139.7, 139.6, 136.5, 135.8, 132.9, 131.4, 129.2, 125.6, 124.3, 123.8, 121.7, 115.6, 115.5 ppm; HRMS (MALDI–TOF, positive) calcd for $C_{14}H_9Br^+$ $[M]^+$ 255.9882, found: 255.9890.

Compound 22: Malononitrile (69 mg, 1.04 mmol) was added to a mixture of **4b** (150 mg, 0.493 mmol) and alumina (2.51 g) in $CHCl_3$ (10 mL). The resulting mixture was stirred at room temperature for 24 h. After removing alumina by filtration, the filtrate was concentrated under reduced pressure to give **22** (170 mg, 98%) as a red solid. M.p. 163 °C; IR (AT-IR): ν_{max} = 2967 (w), 2207 (m), 1547 (s), 1514 (w), 1480 (m), 1459 (s), 1428 (m), 1379 (m), 1363 (m), 1346 (m), 1311 (m), 1273 (m), 1243 (s), 1192 (w), 1174 (w), 1147 (w), 1127 (w), 1077 (m), 1046 (w), 1003 (w), 935 (w), 921 (w), 904 (m), 885 (w), 843 (w), 829 (m), 807 (m), 761 (w), 722 (w), 698 (w), 667 (w), 654 (w), 617 (m) cm^{-1}; UV/Vis (CH_2Cl_2): λ_{max} (log ε) = 275 (4.53), 327 (4.54), 372 (4.11), 389 (4.16), 481 sh (4.26), 507 (4.36) nm; UV/Vis (30% TFA/CH_2Cl_2): λ_{max} (log ε) = 277 (4.33), 328 (4.31), 373 (4.17), 390 (4.16), 513 (4.07) nm; ^{1}H NMR (500 MHz, $CDCl_3$): δ_H = 8.74 (d, *J* = 8.9 Hz, 1H, 5-H), 8.39 (s, 1H, vinyl), 8.35 (d, *J* = 1.7 Hz, 1H, 4-H), 8.29 (d, *J* = 1.4 Hz, 1H, 9-H), 8.07 (d, *J* = 8.6 Hz, 1H, 1-H), 7.91 (dd, *J* = 8.4, 1.9 Hz, 1H, 2-H), 7.75 (d, *J* = 11.2 Hz, 1H, 7-H), 7.65 (t, *J* = 10.9, 8.9 Hz, 1H, 6-H), 3.25 (sept, *J* = 6.9 Hz, 1H, *i*-Pr), 1.45–1.48 (m, 15H, *i*-Pr, *t*-Bu) ppm; ^{13}C NMR (125 MHz, $CDCl_3$): δ_C = 153.3, 149.7, 147.5, 145.0, 144.5, 139.0, 138.0, 134.24, 134.22, 131.7, 131.3, 131.2, 129.2, 120.6, 117.3, 117.1, 115.5, 73.8, 39.8, 35.2, 31.7, 24.5 ppm; HRMS (MALDI–TOF, positive) calcd for $C_{25}H_{24}N_2^+$ $[M]^+$ 352.1934, found 352.1926; HRMS (MALDI–TOF, positive) calcd for $C_{25}H_{24}N_2 + Ag^+$ $[M + Ag]^+$ 459.0985, found 459.0963.

Compound 23a: Piperidine (252 mg, 2.96 mmol) was added to a solution of **4a** (79 mg, 0.30 mmol) and dimethyl malonate (396 mg, 3.00 mmol) in MeOH (5 mL). The resulting mixture

was stirred at room temperature for 18.5 h. The reaction mixture was poured into water, extracted with toluene/EtOAc, washed with brine, and dried with Na_2SO_4. The crude product was purified by column chromatography on silica gel with toluene/AcOEt and reversed phase column chromatography with 80% MeOH to give **23a** (49 mg, 43%) as brown oil. IR (AT-IR): ν_{max} = 2952 (w), 1716 (m), 1587 (m), 1521 (w), 1491 (w), 1465 (m), 1435 (m), 1415 (w), 1364 (w), 1332 (w), 1312 (w), 1255 (s), 1239 (s), 1213 (s), 1160 (w), 1106 (w), 1070 (m), 1038 (w), 992 (w), 921 (w), 890 (w), 825 (w), 805 (w), 748 (m), 710 (w) cm^{-1}; UV/Vis (CH_2Cl_2): λ_{max} (log ε) = 267 (4.29), 313 (4.50), 357 (4.11), 449 (4.07), 575 (2.69), 624 (2.61), 705 sh (2.44) nm; UV/Vis (10% TFA/CH_2Cl_2): λ_{max} (log ε) = 310 (4.63), 392 (4.11), 452 sh (3.82) nm; ^1H NMR (500 MHz, $CDCl_3$): δ_H = 8.59 (s, 1H, vinyl), 8.53 (dd, *J* = 8.6, 0.9 Hz, 1H, 9-H), 8.38 (d, *J* = 1.4 Hz, 1H, 4-H), 8.18 (d, *J* = 10.9 Hz, 1H, 5-H), 7.76–7.82 (m, 2H, 1-H, 2-H), 7.41 (dd, *J* = 10.9, 8.6 Hz, 1H, 7-H), 7.29 (dd, *J* = 10.9, 8.6 Hz, 1H, 8-H), 7.14 (dd, *J* = 10.9, 8.6 Hz, 1H, 6-H), 3.92 (s, 3H, CO_2Me), 3.55 (s, 3H, CO_2Me), 1.47 (s, 9H, *t*-Bu) ppm; ^{13}C NMR (125 MHz, $CDCl_3$): δ_C = 167.6, 166.0, 146.4, 142.6, 140.7, 139.3, 138.6, 136.4, 134.2, 131.1, 129.8, 128.2, 128.0, 126.9, 122.8, 119.5, 119.4, 116.8, 52.6, 52.4, 35.2, 31.9 ppm; HRMS (MALDI–TOF, positive) calcd for $C_{24}H_{24}O_4^+$ $[M]^+$ 376.1669, found 376.1651.

Compound 23b: Piperidine (148 mg, 1.74 mmol) was added to a solution of **4b** (52 mg, 0.17 mmol) and dimethyl malonate (256 mg, 1.94 mmol) in MeOH (5 mL). The resulting mixture was stirred at room temperature for 20 h. The reaction mixture was poured into water, extracted with toluene/EtOAc, washed with brine, and dried with Na_2SO_4. The crude product was purified by column chromatography on silica gel with toluene/AcOEt (4:1) as an eluent to give **23b** (57 mg, 80%) as brown oil. IR (AT-IR): ν_{max} = 2960 (w), 1712 (m), 1637 (w), 1585 (w), 1508 (w), 1469 (m), 1434 (m), 1365 (w), 1303 (w), 1236 (s), 1215 (s), 1191 (m), 1159 (w), 1106 (w), 1072 (m), 1041 (w), 1004 (w), 954 (w), 915 (w), 880 (w), 864 (w), 826 (w), 795 (w), 755 (s), 666 (w) cm^{-1}; UV/Vis (CH_2Cl_2): λ_{max} (log ε) = 250 sh (4.27), 268 (4.35), 291

(4.34), 316 (4.42), 352 (4.18), 378 sh (3.95), 447 (4.00), 582 (2.80), 633 (2.75), 704 sh (2.62), 785 sh (2.44) nm; UV/Vis (10% TFA/CH_2Cl_2): λ_{max} (log ε) = 259 (4.44), 309 (4.58), 385 (4.12), 442 sh (3.87) nm; ^{1}H NMR (500 MHz, $CDCl_3$): δ_H = 8.61 (s, 1H, vinyl), 8.43 (dd, *J* = 8.6, 0.9 Hz, 1H, 5-H), 8.32 (d, *J* = 1.1 Hz, 1H, 4-H), 8.08 (s, 1H, 9-H), 7.77 (dd, *J* = 8.6, 1.7 Hz, 1H, 2-H), 7.72 (d, *J* = 8.3 Hz, 1H, 1-H), 7.38 (d, *J* = 11.5 Hz, 1H, 7-H), 7.27–7.29 (m, 1H, 6-H), 3.94 (s, 3H, CO_2Me), 3.53 (s, 3H, CO_2Me), 3.06 (sept, *J* = 6.9 Hz, 1H, *i*-Pr), 1.45 (s, 9H, *t*-Bu), 1.35 (d, *J* = 6.9 Hz, 6H, *i*-Pr) ppm; ^{13}C NMR (125 MHz, $CDCl_3$): δ_C = 169.2, 146.9, 145.9, 142.3, 140.8, 138.3, 136.7, 136.5, 131.3, 130.8, 128.4, 127.9, 127.8, 120.0, 118.9, 116.7, 113.8, 51.5, 39.3, 35.1, 31.8, 24.0 ppm; HRMS (MALDI–TOF, positive) calcd for $C_{27}H_{30}O_4^+$ $[M]^+$ 418.2139, found 418.2141.

Compound 24a: Piperidine (286 mg, 3.34 mmol) was added to a solution of **6a** (59 mg, 0.29 mmol) in MeOH (5 mL) and dimethyl malonate (333 mg, 2.52 mmol). The resulting mixture was stirred at room temperature for 18.5 h. The reaction mixture was poured into water, extracted with toluene/EtOAc, washed with brine, and dried with Na_2SO_4. The crude product was purified by column chromatography on silica gel with toluene/AcOEt and reversed phase column chromatography with 80% MeOH to give **24a** (42 mg, 46%) as a green solid. M.p. 110–113 °C; IR (AT-IR): ν_{max} = 1734 (m), 1713 (m), 1592 (m), 1489 (w), 1449 (w), 1434 (m), 1353 (w), 1324 (w), 1233 (s), 1213 (s), 1181 (m), 1068 (m), 1042 (w), 990 (w), 947 (w), 932 (w), 907 (w), 881 (w), 849 (w), 766 (m), 753 (m), 691 (m) cm^{-1}; UV/Vis (CH_2Cl_2): λ_{max} (log ε) = 242 sh (4.23), 263 (4.29), 307 (4.46), 360 (4.08), 443 (4.06), 565 (2.71), 615 (2.65), 695 sh (2.40), 773 sh (2.01) nm; UV/Vis (10% TFA/CH_2Cl_2): λ_{max} (log ε) = 305 (4.62), 384 (4.12), 422 sh (3.97) nm; ^{1}H NMR (500 MHz, $CDCl_3$): δ_H = 8.59 (s, 1H, vinyl), 8.51 (dd, *J* = 8.6, 0.9 Hz, 1H, 9-H), 8.39 (d, *J* = 8.0 Hz, 1H, 1-H), 8.19 (d, *J* = 11.2 Hz, 1H, 5-H), 7.83 (d, *J* = 8.0 Hz, 1H, 4-H), 7.70–7.73 (m, 1H, 3-H), 7.52–7.55 (m, 1H, 2-H), 7.41–7.45 (m, 1H, 7-H), 7.30 (dd, *J* = 10.9, 8.6 Hz, 1H, 8-H), 7.18 (dd, *J* = 10.6, 8.9 Hz, 1H, 6-H), 3.92 (s, 3H,

CO_2Me), 3.53 (s, 3H, CO_2Me) ppm; ^{13}C NMR (125 MHz, $CDCl_3$): δ_C = 167.3, 165.8, 142.3, 140.5, 140.3, 139.1, 136.4, 134.1, 131.1, 130.1, 129.5, 128.4, 127.2, 123.2, 123.1, 121.0, 119.6, 119.5, 52.6, 52.3 ppm; HRMS (MALDI–TOF, positive) calcd for $C_{20}H_{16}O_4^+$ $[M]^+$ 320.1043, found 320.1021; HRMS (MALDI–TOF, positive) calcd for $C_{20}H_{16}O_4 + Ag^+$ $[M + Ag]^+$ 427.0094, found 427.0071.

Compound 24b: Piperidine (337 mg, 3.96 mmol) was added to a solution of **6b** (98 mg, 0.40 mmol) and dimethyl malonate (518 mg, 3.92 mmol) in MeOH (10 mL). The resulting mixture was stirred at room temperature for 20.5 h. The reaction mixture was poured into K_2CO_3 aq., extracted with toluene/AcOEt, washed with brine, and dried with Na_2SO_4. The crude product was purified by column chromatography on silica gel with toluene/AcOEt and reversed phase column chromatography with 80% MeOH to give **24b** (100 mg, 70%) as brown oil. IR (AT-IR): ν_{max} = 2956 (w), 1713 (m), 1600 (w), 1579 (m), 1505 (w), 1482 (w), 1459 (w), 1433 (m), 1364 (w), 1315 (w), 1235 (s), 1215 (s), 1187 (m), 1159 (w), 1133 (w), 1072 (m), 1048 (w), 986 (w), 941 (w), 895 (w), 860 (w), 829 (w), 803 (w), 760 (s), 723 (w) cm^{-1}; UV/Vis (CH_2Cl_2): λ_{max} (log ε) = 246 sh (4.22), 265 (4.30), 311 (4.45), 360 (4.03), 449 (4.06), 560 (2.79), 629 (2.72), 694 sh (2.51) nm; UV/Vis (10% TFA/CH_2Cl_2): λ_{max} (log ε) = 304 (4.55), 378 (4.09), 420 sh (3.95) nm; ^1H NMR (500 MHz, $CDCl_3$): δ_H = 8.61 (s, 1H, vinyl), 8.38 (dd, *J* = 8.5, 0.9 Hz, 1H, 5-H), 8.31 (d, *J* = 8.0 Hz, 1H, 1-H), 8.09 (s, 1H, 9-H), 7.79 (d, *J* = 8.0 Hz, 1H, 4-H), 7.68 (t, *J* = 8.0 Hz, 1H, 3-H), 7.47 (t, *J* = 8.0 Hz, 1H, 2-H), 7.40 (d, *J* = 11.4 Hz, 1H, 7-H), 7.30 (dd, *J* = 11.4, 8.5 Hz, 1H, 6-H), 3.93 (s, 3H, CO_2Me), 3.51 (s, 3H, CO_2Me), 3.04–3.09 (sept, *J* = 13.5, 1H, *i*-Pr), 1.35 (d, *J* = 6.9 Hz, 6H, *i*-Pr) ppm; ^{13}C NMR (125 MHz, $CDCl_3$): δ_C = 167.5, 166.1, 148.0, 142.4, 140.8, 140.4, 139.6, 136.7, 131.8, 131.0, 129.4, 129.2, 128.2, 122.8, 122.3, 120.9, 119.4, 119.0, 52.6, 52.2, 39.2, 23.9 ppm; HRMS (MALDI–TOF, positive) calcd for $C_{23}H_{22}O_4^+$ $[M]^+$ 362.1513, found 362.1510; HRMS (MALDI–TOF, positive) calcd for $C_{23}H_{22}O_4 + Ag^+$ $[M + Ag]^+$ 469.0564, found 470.0541.

Compound 25: A solution of **24b** (42 mg, 0.13 mmol) in Eaton's reagent (3 mL) was stirred at 70 °C for 2 days. After cooling to room temperature, the reaction mixture was poured into brine, extracted with $CHCl_3$/EtOAc, and dried with Na_2SO_4. The crude product was purified by silica gel column chromatography with EtOAc as an eluent to give **25** (25 mg, 66%) as a red solid. M.p. 133 °C ; IR (AT-IR): ν_{max} = 1712 (m), 1681 (w), 1624 (m), 1605 (w), 1574 (m), 1543 (s), 1498 (m), 1438 (m), 1416 (m), 1389 (m), 1338 (m), 1304 (m), 1261 (m), 1240 (m), 1214 (s), 1114 (m), 1065 (m), 1012 (m), 976 (w), 876 (w), 863 (w), 774 (m), 740 (m), 706 (m), 695 (m), 680 (m), 663 (w) cm^{-1}; UV/Vis (CH_2Cl_2): λ_{max} (log ε) = 272 (3.98), 281 (4.02), 312 (4.15), 328 sh (4.15), 337 (4.19), 366 (4.11), 383 (4.19), 455 sh (3.81), 488 (4.17), 522 (4.32) nm; UV/Vis (10% TFA/CH_2Cl_2): λ_{max} (log ε) = 271 (4.10), 289 (3.81), 340 (4.27), 351 (4.26), 481 (4.27) nm; ^{1}H NMR (500 MHz, $CDCl_3$): δ_H = 8.91 (s, 1H, 1-H), 8.66–8.70 (m, 2H, 4-H, 11-H), 8.53–8.57 (m, 2H, 6-H, 7-H), 7.85 (t, *J* = 7.6 Hz, 1H, 5-H), 7.67–7.71 (m, 1H, 9-H), 7.60–7.54 (m, 2H, 8-H, 10-H), 3.99 (s, 3H, CO_2Me) ppm; ^{13}C NMR (125 MHz, $CDCl_3$): δ_C = 181.3, 168.0, 146.7, 145.7, 140.0, 139.0, 136.8, 135.0, 134.3, 132.8, 132.3, 130.2, 129.4, 127.9, 126.9, 125.8, 125.5, 117.8, 52.4 ppm; HRMS (MALDI–TOF, positive) calcd for $C_{19}H_{12}O_3$ + H^+ $[M + H]^+$ 289.0859, found 289.0852.

Synthesis of 25 with PPA: A solution of **24a** (77 mg, 0.24 mmol) in PPA (10 mL) was stirred at 95 °C for 11 h. After cooling to room temperature, the reaction mixture was poured into brine, extracted with $CHCl_3$/EtOAc, and dried with Na_2SO_4. The crude product was purified by silica gel column chromatography with EtOAc as an eluent to give **25** (25 mg, 36%) as a red solid.

ASSOCIATED CONTENT

Supporting Information

Copies of ^{1}H, ^{13}C NMR, COSY spectra, HRMS, UV/Vis and fluorescent spectra, and cyclic and differential pulse voltammograms of reported compounds. This material is available free of charge *via* the Internet at http://pubs.acs.org.

AUTHOR INFORMATION

Corresponding Author

*E-mail: tshoji@shinshu-u.ac.jp

ORCID

Taku Shoji: 0000-0001-8176-2389

Tetsuo Okujima: 0000-0002-6552-2606

Shunji Ito: 0000-0002-1627-2583

NOTES

The authors declare no competing financial interest.

Professor Masafumi Yasunami passed away on January 25, 2013.

ACKNOWLEDGMENTS

This work was supported by JSPS KAKENHI Grant Number 17K05780 and 21K05037. Part of this study was also supported by emeritus professor Hiroshi Kato (Shinshu University).

REFERENCES

1 (a) Berresheim, A. J.; Müller, M.; Müllen, K. Polyphenylene Nanostructures, *Chem. Rev.* **1999**, *99*, 1747–1786; (b) Sun, Z.; Ye, Q.; Chi, C.; Wu, J. Low band gap polycyclic hydrocarbons: from closed-shell near infrared dyes and semiconductors to open-shell

radicals, *Chem. Soc. Rev.* **2012**, *41*, 7857–7889; (b) Hopf, H. Pentalenes - From Highly Reactive Antiaromatics to Substrates for Material Science, *Angew. Chem. Int. Ed.* **2013**, *52*, 12224–12226; (c) Kubo, T. Phenalenyl-Based Open-Shell Polycyclic Aromatic Hydrocarbons, *Chem. Rec.* **2015**, *15*, 218–232; (d) Hirai, M.; Tanaka, N.; Sakai, M.; Yamaguchi, S. Structurally constrained boron-, nitrogen-, silicon-, and phosphorus-centered polycyclic π-conjugated systems, *Chem. Rev.* **2019**, *119*, 8291–8331; (d) Dhbaibi, K.; Favereau, L.; Crassous, J. Enantioenriched Helicenes and Helicenoids Containing Main-Group Elements (B, Si, N, P), *Chem. Rev.* **2019**, *119*, 8846–8953; (e) Borissov, A.; Maurya, Y. K.; Moshniaha, L.; Wong, W.-S.; Żyła-Karwowska, M.; Stępień, M. Recent Advances in Heterocyclic Nanographenes and Other Polycyclic Heteroaromatic Compounds, *Chem. Rev.* **2021** (DOI: 10.1021/acs.chemrev.1c00449).

2 (a) Fischer, G. Azulenes Fused to Heterocycles, *Adv. Heterocycl. Chem.* **2009**, *97*, 131–218; (b) Shoji, T.; Ito, S. The Preparation and Properties of Heteroarylazulenes and Hetero-Fused Azulenes, *Adv. Heterocyclic Chem.* **2018**, *126*, 1–54; (c) Shoji, T.; Okujima, T.; Ito, S. Development of Heterocycle-Substituted and Fused Azulenes in the Last Decade (2010–2020), *Int. J. Mol. Sci.* **2020**, *21*, 7087.

3 (a) Yamaguchi, Y.; Maruya, Y.; Katagiri, H.; Nakayama, K.-i.; Ohba, Y. Synthesis, Properties, and OFET Characteristics of 5,5'-Di(2-azulenyl)-2,2'-bithiophene (DAzBT) and 2,5-Di(2-azulenyl)-thieno[3,2-*b*]thiophene (DAzTT), *Org. Lett.* **2012**, *14*, 2316–2319; (b) Yamaguchi, Y.; Ogawa, K.; Nakayama, K.-i.; Ohba, Y.; Katagiri, H. Terazulene: A High-Performance n-Type Organic Field-Effect Transistor Based on Molecular Orbital Distribution Control, *J. Am. Chem. Soc.* **2013**, *135*, 19095–19098; (c) Yao, J.; Cai, Z.; Liu, Z.; Yu, C.; Luo, H.; Yang, Y.; Yang, S.; Zhang, G.; Zhang, D. Tuning the Semiconducting Behaviors of New Alternating Dithienyldiketopyrrolopyrrole–Azulene Conjugated Polymers by Varying the Linking Positions of Azulene, *Macromolecules* **2015**, *48*, 2039–2047; (d) Yamaguchi, Y.; Takubo, M.; Ogawa, K.; Nakayama, K.-i.; Koganezawa, T.; Katagiri, H. Terazulene Isomers: Polarity Change of OFETs through Molecular Orbital Distribution Contrast, *J. Am. Chem. Soc.* **2016**, *138*, 11335–11343.

4 (a) Puodziukynaite, E.; Wang, H.-W.; Lawrence, J.; Wise, A. J.; Russell, T. P.; Barnes, M. D.; Emrick, T. Azulene Methacrylate Polymers: Synthesis, Electronic Properties, and Solar Cell Fabrication, *J. Am. Chem. Soc.* **2014**, *136*, 11043–11049; (b) Nishimura, H.; Ishida, N.; Shimazaki, A.; Wakamiya, A.; Saeki, A.; Scott, L. T.; Murata, Y. Hole-Transporting Materials with a Two-Dimensionally Expanded π-System around an Azulene Core for Efficient

Perovskite Solar Cells, *J. Am. Chem. Soc.* **2015**, *137*, 15656–15659; (c) Chen, Y.; Zhu, Y.; Yang, D.; Zhao, S.; Zhang, L.; Yang, L.; Wu, J.; Huang, Y.; Xu, Z.; Lu, Z. An Azulene-Containing Low Bandgap Small Molecule for Organic Photovoltaics with High Open Circuit Voltage, *Chem. Eur. J.* **2016**, *22*, 14527–14530; (d) Cowper, P.; Pockett, A.; Kociok-Kohn, G.; Cameron, P. J.; Lewis, S. E. Azulene - Thiophene - Cyanoacrylic acid dyes with donor-π-acceptor structures. Synthesis, characterization and evaluation in dye-sensitized solar cells. *Tetrahedron* **2018**, *74*, 2775–2786; (e) Tzoganakis, N.; Feng, B.; Loizos, M.; Krassas, M.; Tsikritzis, D.; Zhuang, X.; Kymakis, E. Ultrathin PTAA interlayer in conjunction with azulene derivatives for the fabrication of inverted perovskite solar cells, *J. Mater. Chem. C* **2021**, *9*, 14709–14719; (f) Yang, L.; Zhu, Y.; Liu, J.; Chen, Y.; Wu, J.; Pang, Z.; Lu, Z.; Zhao, S.; Huang, Y. Marked effects of azulenyl vs. naphthyl groups on donor-π-acceptor-π-donor small molecules for organic photovoltaic cells, *Dyes and Pigm.* **2021**, *187*, 109079; (g) Raheem, A. A.; Murugan, P.; Shanmugam, R.; Praveen, C. Azulene Bridged π-Distorted Chromophores: The Influence of Structural Symmetry on Optoelectrochemical and Photovoltaic Parameters, *ChemPlusChem* **2021**, *86*, 1451–1460.

5 (a) Ito, S.; Morita, N. Creation of stabilized electrochromic materials by taking advantage of azulene skeletons, *Eur. J. Org. Chem*. **2009**, 4567–4579; (b) Ito, S.; Shoji, T.; Morita, N. Recent advances in the development of methods for the preparation of functionalized azulenes for electrochromic applications, *Synlett*, **2011**, 2279–2298; (c) Shoji, T.; Ito, S. Azulene-based donor-acceptor systems: synthesis, optical, and electrochemical properties, *Chem. Eur. J.* **2017**, *23*, 16696–16709.

6 (a) Murai, M.; Iba, S.; Ota, H.; Takai, K. Azulene-Fused Linear Polycyclic Aromatic Hydrocarbons with Small Bandgap, High Stability, and Reversible Stimuli Responsiveness, *Org. Lett.* **2017**, *19*, 5585–5588; (b) Poronik, Y. M.; Mazur, L. M.; Samoc, M.; Jacquemin, D.; Gryko, D. T. 2,5-Bis(azulenyl)pyrrolo[3,2-*b*]pyrroles - the key influence of the linkage position on the linear and nonlinear optical properties, *J. Mater. Chem. C* **2017**, *5*, 2620–2628; (c) Lopez-Alled, C. M.; Sanchez-Fernandez, A.; Edler, K. J.; Sedgwick, A. C.; Bull, S. D.; McMullin, C. L.; Kociok-Kohn, G.; James, T. D.; Wenk, J.; Lewis, S. E. Azulene-boronate esters: colorimetric indicators for fluoride in drinking water, *Chem. Commun.* **2017**, *53*, 12580–12583; (d) Murfin, L. C.; Weber, M.; Park, S.-J.; Kim, W.-T.; Lopez-Alled, C. M.; McMullin, C. L.; Pradaux-Caggiano, F.; Lyall, C. L.; Kociok-Kohn, G.; Wenk, J.; Bull, S. D.; Yoon, J.; Kim, H. M.; James, T. D.; Lewis, S. E. Azulene-Derived Fluorescent Probe for Bioimaging: Detection of Reactive Oxygen and Nitrogen Species by Two-Photon Microscopy,

J. Am. Chem. Soc. **2019**, *141*, 19389–19396.

7 (a) Binsch, G.; Heilbronner, E.; Jankow, R.; Schmidt, D. Fluorescence anomaly of azulene, *Chem. Phys. Lett.* **1967**, *1*, 135–138; (b) Otteson, D.; Jutz, C.; Michl, J. Magnetic circular dichroism of cyclic π-electron systems. 15. Benzazulenes, *J. Am. Chem. Soc.* **1978**, *100*, 6882–6883; (c) Gupta, A. D; Chatterjee, S.; Gupta, N. K. D. Theoretical studies of some nonbenzenoid hydrocarbons. V. Benzazulenes and benzofluoranthenes, *Bull. Chem. Soc. Jpn.* **1979**, *52*, 3070–3075; (d) Yamaguchi, H.; Ninomiya, K.; Fukuda, M.; Muraoka, T. Magnetic circular dichroism and anomalous fluorescence spectra of benz[*a*]azulene and naphth[2,1-*a*]azulene, *Spectrochim. Acta,* **1980**, *36A*, 1003–1005; (e) Higashi, M.; Yamaguchi, H.; Schmidt, W. Photoelectron spectra of benzazulenes, *J. Chem. Soc. Faraday Trans. 2* **1987**, *83*, 741–745; (f) Awuku, S.; Bradley, S. J.; Ghiggino, K. P.; Steer, R. P.; Stevens, A. L.; White, J. M.; Yeow, C. Photophysics and spectroscopy of 1,2-Benzazulene, *Chem. Phys. Lett.* **2021**, *784*, 139114.

8 (a) Jutz, C.; Schweiger, E. Simple synthesis of pyraceheptylene and benzo[*a*]pyraceheptylene, *Angew. Chem. Int. Ed. Eng.* **1971**, *10*, 808–809; (b) Jutz, C.; Schweiger, E. Darstellung von Benzazulenen aus Azulenderivaten, *Chem. Ber.* **1974**, *107*, 2383–2396; (c) Hafner, K.; Diehl, H.; Richarz, W. Cycloaddition reactions of aceheptylene-a simple synthesis of dicyclopent[*ef*,*kl*]heptalenes, *Angew. Chem.* **1976**, *88*, 125–126; (d) Yamamoto, K.; Murata, I. The cyclohept[*a*]acenaphthylenylium ion, *Angew. Chem.* **1976**, *88*, 262; (e) Mizumoto, K.; Okada, K.; Oda, M. Generation and notable position dependent electrocyclization of cycloheptatrienylphenylcarbonium ions -electrocyclization of a norcaradiene, *Tetrahedron Lett.* **1984**, *25*, 2999–3002; (f) Fukazawa, Y.; Aoyagi, M.; Ito, S. Naphtho[1,8-*ab*:4,5-*a*'*b*']diazulene, the first nonalternant isomer of dibenzopyrene, *Tetrahedron Lett.* **1981**, *22*, 3879–3882; (g) Toda, T.; Minabe, M.; Yoshida, M.; Tobita, K. Electrophilic substitution reactions of benz[*a*]indeno[1,2,3-*cd*]azulene, *J. Org. Chem.* **1990**, *55*, 1297–1300; (h) Linden, A.; Mever, M.; Mohler, P.; Rippert, A. J.; Hansen, H.-J. A detailed investigation of the reaction of 5,9-diphenylbenz[*a*]azulene with dialkyl acetylenedicarboxylates leading to dialkyl 8,12-diphenylbenzo[*a*]heptalene-6,7-dicarboxylates, *Helv. Chim. Acta* **1999**, *82*, 2274–2315; (i) Kuwatani, Y.; Yoshida, T.; Kusaka, A.; Oda, M.; Hara, K.; Yoshida, M.; Matsuyama, H.; Iyoda, M. Synthesis of benzocyclobutadiene trimers and *all-Z*-tribenzo[12]annulene. A new

family of concave π-systems, *Tetrahedron* **2001**, *57*, 3567–3576; (j) Wu, C.-P.; Devendar, B.; Su, H.-C.; Chang, Y.-H.; Ku, C.-K. Efficient synthesis and applications of 2-substituted azulene derivatives: towards highly functionalized carbo- and heterocyclic molecules, *Tetrahedron Lett.* **2012**, *53*, 5019–5022; (k) Yamamoto, K.; Ie, Y.; Tohnai, N.; Kakiuchi, F.; Aso, Y. Antiaromatic character of cycloheptatriene-bis-annelated indenofluorene framework mainly originated from heptafulvene segment, *Sci. Rep.* **2018**, *8*, 17663.

9 Plattner, P. A.; Fürst, A.; Chopin, J.; Winteler, G. Zur Kenntnis der Sesquiterpene. 81. Mitteilung. 1,2-Benz-azulen, *Helv. Chim. Acta* **1948**, *31*, 501–504.

10 Treibs, W. Über bi- und polycyclische Azulene, I. Mitteil.: Synthese des 1.2-Benz-azulens, *Chem. Ber.* **1948**, *81*, 38–41.

11 Cresp, T. M.; Wege, D. The addition of benzyne to azulene, *Tetrahedron* **1986**, *42*, 6713–6718.

12 O'Leary, M. A.; Wege, D. The addition of benzocyclobutenylidene to benzene. A novel route to benz[a]azclene, *Tetrahedron Lett.* **1978**, *19*, 2811–2814.

13 Sperandio, D.; Hansen, H.-J. An Efficient Straightforward Synthesis of Benz[*a*]azulene

An Analysis of the Bonding Properties of Benz[a]azulene by X-Ray, NMR, and Computational Studies, *Helv. Chim. Acta* **1995**, *78*, 765–771.

14 Bühl, M.; Koźmiński, W.; Linden, A.; Nanz, D.; Sperandio, D.; Hansen, H.-J. An Analysis of the Bonding Properties of Benz[a]azulene by X-Ray, NMR, and Computational Studies, *Helv. Chim. Acta* **1996**, *79*, 837–854.

15 Amemiya, T.; Yasunami, M.; Takase, K. The novel oxidation of 1-alkylazulenes to 1-acylazulenes with DDQ, *Chem. Lett.* **1977**, *6*, 587–590.

16 (a) Nozoe, T.; Takase, K.; Tada, M. Synthesis of 5- and 6-acetylazulene derivatives, *Bull. Chem. Soc. Jpn.* **1963**, *36*, 1010–1016; (b) Nozoe, T.; Takase, K.; Tada, M. Anionoid substitution reaction of diethyl 6-bromoazulene-1,3-dicarboxylate, *Bull. Chem. Soc. Jpn.* **1965**, *38*, 247–251; (c) Schenk, G. H.; Fryer, P. A. Use of the molecular orbital theory of charge transfer spectra in searching for multiple charge transfer bands of the Pi complexes of 2,3-dichloro-5,6-dicyano-p-benzoquinone, *Anal. Chem.* **1970**, *42*, 1694–1698; (d) Takase, K.; Nozoe, T.; Nakazawa, T.; Fukuda, S. Formation of azulene derivatives from 2*H*-Cyclohepta[*b*]furan-2-one derivatives, *Tetrahedron* **1971**, *27*, 3357–3368; (e) Nozoe, T.; Takase, K.; Fukuda, S. Synthesis of 1-phenylazulene and 2-phenylazulene from the troponoid compound, *Bull. Chem. Soc. Jpn.* **1971**, *44*, 2210–2213.

17 Shoji, T.; Ito, S.; Yasunami, M. Synthesis of Azulene Derivatives from 2*H*-Cyclohepta[*b*]furan-2-ones as Starting Materials: Their Reactivity and Properties Int. *J. Mol. Sci.* **2021**, *22*, 10686.

18 Ikegai, K.; Imamura, M.; Suzuki, T.; Nakanishi, K.; Murakami, T.; Kurosaki, E.; Noda, A.; Kobayashi, Y.; Yokota, M.; Koide, T.; Kosakai, K.; Ohkura, Y.; Takeuchi, M.; Tomiyama, H.; Ohta, M. Synthesis and biological evaluation of C-glucosides with azulene rings as selective SGLT2 inhibitors for the treatment of type 2 diabetes mellitus: Discovery of YM543, *Bioorg. Med. Chem.* **2013**, *21*, 3934–3948.

19 (a) Ito, S.; Kubo, T.; Morita, N.; Ikoma, T.; Tero-Kubota, S.; Tajiri, A. Synthesis, Stabilities, and Redox Behavior of Di(1-azulenyl)(6-azulenyl)methylium Hexafluorophosphates. Generation of a Donor-Acceptor-Substituted Neutral Radical by Azulenes, *J. Org. Chem.* **2003**, *68*, 9753–9762; (b) Ito, S.; Akimoto, K.; Kawakami, J.; Tajiri, A.; Shoji, T.; Satake, H.; Morita, N. Synthesis, stabilities, and redox behavior of mono-, di-, and tetracations composed of di(1-azulenyl)methylium units connected to a benzene ring by phenyl- and 2-thienylacetylene spacers. A concept of a cyanine-cyanine hybrid as a stabilized electrochromic system, *J. Org. Chem.* **2007**, *72*, 162–172.

20 Shoji, T.; Higashi, J.; Ito, S.; Toyota, K.; Asao, T.; Yasunami, M.; Fujimori, K.; Morita, N. Synthesis and Redox Behavior of 1-Azulenyl Sulfides and Efficient Synthesis of 1,1'-Biazulenes, *Eur. J. Org. Chem*. **2008**, 1242–1252.

21 Texier-Boullet, F.; Foucaud, A. Knoevenagel condensation catalyzed by aluminum oxide, *Tetrahedron Lett.* **1982**, *23*, 4927–4928.

22 Yamamura, K.; Kitagawa, Y.; Hashimoto, M. Crystal Structure of 1,1,1-Triphenyl-4-(10-benz[*a*]azulenyl)-3,4-buten-2-one, *Anal. Sci.* **2002**, *18*, 373–374.

23 CCDC 1959815 (**6b**) contains the supplementary crystallographic data for this paper. These data are provided free of charge by The Cambridge Crystallographic Data Centre.

24 (a) Plattner, P. A.; Pfau, A. S. Zur Kenntnis der flüchtigen Pflanzenstoffe V. Über die Darstellung des Grundkörpers der Azulen-Reihe, *Helv. Chim. Acta* **1937**, *20*, 224–232; (b) Plattner, P. A.; Roniger, H. Zur Kenntnis der Sesquiterpene. (58. Mitteilung). 4,8-Dimethyl-6-isopropyl-azulen, *Helv. Chim. Acta* **1943**, *26*, 905–912; (c) Plattner, P. A.; Fürst, A. Zur Kenntnis der Sesquiterpene. (66. Mitteilung). Über den Einfluss der Substitution auf die Farbe der Azulene; 2-Äthyl-azulen, *Helv. Chim. Acta* **1945**, *28*, 1636–1638; (d) Plattner, P. A.; Fürst, A.; Schmid, H. Zur Kenntnis der Sesquiterpene. (67. Mitteilung). Über den Einfluss der Substitution auf die Farbe der Azulene;

1,3,4,8-Tetramethyl-azulen, *Helv. Chim. Acta* **1945**, *28*, 1647–1651; (e) Plattner, P. A.; Heilbronner, E. Zur Kenntnis der Sesquiterpene. (76. Mitteilung). Die Absorptionskurven des Azulens und der fünf Monomethyl-azulene im sichtbaren Bereich, *Helv. Chim. Acta* **1947**, *30*, 910–920; (f) Plattner, P. A.; Heilbronner, E.; Fürst, A. Zur Kenntnis der Sesquiterpene. 78. Mitteilung. Die spektroskopische Prüfung verschiedener Präparate von 5-Methyl-azulen, *Helv. Chim. Acta* **1947**, *30*, 1100–1105; (g) Plattner, P. A.; Fürst, A.; Jirasek, K. Zur Kenntnis der Sesquiterpene. (79. Mitteilung). Im Fünfring mehrfach substituierte Azulene, *Helv. Chim. Acta* **1947**, *30*, 1320–1329.

25 (a) Reid, D. H.; Stafford, W. H.; Stafford, W. L.; McLennan, G.; Voigt, A. The azulene series. III. The synthesis and properties of 3-benzylideneguaiazulenium chloride, *J. Chem. Soc.* **1958**, 1110–1117; (b) Kirby, E. C.; Reid, D. H. Conjugated cyclic hydrocarbons and their heterocyclic analogs. II. Condensation of azulenes with homocyclic and heterocyclic aromatic aldehydes in the presence of perchloric acid, *J. Chem. Soc.* **1960**, 494–501; (c) Amir, E.; Amir, R. J.; Campos, L. M.; Hawker, C. J. Stimuli-Responsive Azulene-Based Conjugated Oligomers with Polyaniline-like Properties, *J. Am. Chem. Soc.* **2011**, *133*, 10046–10049; (d) Murai, M.; Ku, S.-Y.; Treat, N. D.; Robb, M. J.; Chabinyc, M. L.; Hawker, C. J. Modulating structure and properties in organic chromophores: influence of azulene as a building block, *Chem. Sci.* **2014**, *5*, 3753–3760.

26 (a) Wurzer, A. J.; Wilhelm, T.; Piel, J.; Riedle, E. Comprehensive measurement of the S1 azulene relaxation dynamics and observation of vibrational wavepacket motion, *Chem. Phys. Lett.* **1999**, *299*, 296–302; (b) Kim, S. Y.; Lee, G. Y.; Han, S. Y.; Lee, M. Fluorescence quenching dynamics of azulene and 2-haloazulenes by CCl4 in nonpolar solvents, *Chem. Phys. Lett.* **2000**, *318*, 63–68.

27 (a) Amir, E.; Amir, R. J.; Campos, L. M.; Hawker, C. J. Stimuli-responsive azulene-based conjugated oligomers with polyaniline-like properties, *J. Am. Chem. Soc.* **2011**, *133*, 10046–10049; (b) Koch, M.; Blacque, O.; Venkatesan, K. Syntheses and Tunable Emission Properties of 2-Alkynyl Azulenes, *Org. Lett.* **2012**, *14*, 1580–1583; (c) Zhou, Y.; Zhuang, Y.; Li, X.; Ågren, H.; Yu, L.; Ding, J.; Zhu, L. Selective Dual-Channel Imaging on Cyanostyryl-Modified Azulene Systems with Unimolecularly Tunable Visible–Near Infrared Luminescence, *Chem. Eur. J.* **2017**, *23*, 7642–7647.

28 Yamaguchi, H.; Sato, S.; Yasunami, M.; Sato, T.; Yoshinobu, M. Anomalous fluorescence spectra of benz[*a*]azulene derivatives, *Spectrochimica Acta Part A* **1997**, *53*, 2471–2473.

29 Ito, S.; Nomura, A.; Morita, N.; Kabuto, C.; Kobayashi, H.; Maejima, S.; Fujimori, K.;

Yasunami, M. Synthesis and Two-Electron Redox Behavior of Diazuleno[2,1-*a*:1,2-*c*]naphthalenes, *J. Org. Chem.* **2002**, *67*, 7295–7302.